Contemporary Problems in Architecture and Construction

Edited by
Darja Kubečková

TRANS TECH PUBLICATIONS

Contemporary Problems in Architecture and Construction

Edited by
Darja Kubečková

Contemporary Problems in Architecture and Construction

Selected, peer reviewed papers from the
6th International Conference on
Contemporary Problems of Architecture and Construction,
June 24-27, 2014, Ostrava, Czech Republic

Edited by

Darja Kubečková

Trans Tech Publications Ltd
Churerstrasse 20
CH-8808 Pfaffikon
Switzerland
http://www.ttp.net

Volume 1020 of
Advanced Materials Research
ISSN print 1022-6680
ISSN cd 1022-6680
ISSN web 1662-8985

Full text available online at *http://www.scientific.net*

***Distributed** worldwide by*

Trans Tech Publications Ltd
Churerstrasse 20
CH-8808 Pfaffikon
Switzerland

Fax: +41 (44) 922 10 33
e-mail: sales@ttp.net

and in the Americas by

Trans Tech Publications Inc.
PO Box 699, May Street
Enfield, NH 03748
USA

Phone: +1 (603) 632-7377
Fax: +1 (603) 632-5611
e-mail: sales-usa@ttp.net

Preface

We are pleased to welcome you to the conference book of the 6th International Conference on Contemporary Problems of Architecture and Construction held on 24th – 27th June 2014 at Faculty of Civil Engineering, VŠB - Technical University of Ostrava, Czech Republic.

It is my pleasure to announce the participation of expert speakers from various countries in this four-day event. We have received scientific papers from distinguished universities and organizations from various countries. This is really a unique platform for all researchers to discuss and exchange experiences.

I would like to thank all authors of submitted papers for their participation. They contributed a great deal of effort and creativity to produce this work. I am happy they chose the 6th International Conference on Contemporary Problems of Architecture and Construction, as the place to present it. Thanks also go to the editors and reviewers, who donated substantial time from their busy schedules to carefully read and evaluate the submitted scientific papers.

In addition, the Organizing Committee would like to take this opportunity to extend our sincere gratitude to all supporting organizations and universities for their support and encouragement and got making the event a success.

Prof. Darja Kubečková, MSc., Ph.D.
Guarantor of the Conference
VŠB - Technical University of Ostrava, Czech Republic

Partner Universities

- **National University of Architecture and Construction of Armenia**
- **Beijing University of Civil Engineering and Architecture**
- **Czestochowa University of Technology**
- **Saint-Petersburg State University of Architecture and Civil Engineering**
- **VŠB – Technical University of Ostrava, Faculty of Civil Engineering**

International Scientific Committee

Organizing Committee

- **Prof. Chengzhi Qi, MSc.**
  Beijing University of Civil Engineering and Architectue, China
- **Prof. Jaroslaw Rajczyk**
  MSc., Czestochowa University of Technology, Poland
- **Prof. dr hab. inż. Yuri Safaryan,**
  Yerevan State university of Architecture and Construction, Armenia
- **Prof. dr hab. inż. Arestak Sarukhanyan**
  Yerevan State university of Architecture and Construction, Armenia
- **Prof. Yevgeni Smirnov, MSc.**
  Saint Petersburg State University of Architecture and Civil Engineering, Russia
- **Prof. dr hab. inż. Hovhannes Tokmajyan**
  Yerevan State university of Architecture and Construction, Armenia
- **Prof. Vardges Yedoyan, MSc.**
  Yerevan State university of Architecture and Construction, Armenia
- **Assoc. Prof. Karel Kubečka, MSc., Ph.D.**
  VŠB - Technical University of Ostrava, Czech Republic
- **Assoc. Prof. Karel Vojtasík, MSc., CSc.**
  VŠB - Technical University of Ostrava, Czech Republic
- **Marcela Halířová, MSc., Ph.D.**
  VŠB - Technical University of Ostrava, Czech Republic
- **Marek Jašek, MSc., Ph.D.**
  VŠB - Technical University of Ostrava, Czech Republic
- **Zdeněk Peřina, MSc., Ph.D.**
  VŠB - Technical University of Ostrava, Czech Republic
- **Pavel Vlček, MSc., Ph.D.**
  VŠB - Technical University of Ostrava, Czech Republic
- **David Hibler, MSc.**
  VŠB - Technical University of Ostrava, Czech Republic
- **Barbora Hrubá, MSc.**
  VŠB - Technical University of Ostrava, Czech Republic
- **Petr Waldstein, MSc.**
  VŠB - Technical University of Ostrava, Czech Republic
- **Jiří Winkler, MSc.**
  VŠB - Technical University of Ostrava, Czech Republic
- **Pavla Šimelová, B.A.**
  VŠB - Technical University of Ostrava, Czech Republic
- **Radim Pientka**
  VŠB - Technical University of Ostrava, Czech Republic

Table of Contents

Chapter 1: Materials and Technologies in Civil and Building Engineering

Chapter 2: Structural Mechanics and Analysis, Applied Mechanics, Constructions and Civil Engineering Applications

Chapter 3: Geotechnologies and Geology, Tunneling and Subways, Seismology

Chapter 4: Environmental Engineering, Green, Energy and Thermal Engineering in Building

Chapter 5: Architectural Culture and Design, Urban and Transport Planning and Problems

Chapter 6: Municipal Engineering, Water Systems and Resources, Management and Economics, Forensic Sciences

CHAPTER 1:

Materials and Technologies in Civil and Building Engineering

Advanced Materials Research Vol. 1020 (2014) pp 3-8

doi:10.4028/www.scientific.net/AMR.1020.3

Development of green engineered cementitious composites

Marek Jašek[1,a*], Jiří Brožovský[1,b], Lucie Mynarzová[1,c] and Jan Hurta[1,d]

[1] VSB-TU of Ostrava, Faculty of Civil Engineering, L. Podéště 1875, 708 00, Ostrava-Poruba, Czech Republic

[a*]marek.jasek@vsb.cz, [b]jiri.brozovsky@vsb.cz, [c]lucie.mynarzova@vsb.cz, [d]jan.hurta@vsb.cz,

Keywords: Engineered cementitious composites, fiber, fly ash, interface, matrix.

Abstract: A development of fiber-cement composites is often focused on cost-effective and environmentally friendly materials (so-called green materials). Production of this material should produce less waste and it also should use less energy and less natural sources. There are numerous approaches to the development of green composites. One of the possible ways is a utilization of fly ashes instead of the cement part of composite.

The paper discusses a development of green cementitious composite which incorporated fly ash materials produced in the Moravian-Silesian region as a partial replacement of the cement part of the composite.

Introduction

In recent years, we are able to find many different types of concrete or rather composites, which are relativity different from normal concrete. Engineered cementitious composite (ECC) is very ductile fine concrete (mortar) with a matrix on the basic of portland cement reinforced with short fibers. ECC represents new generation of high performance concrete and also called as flexible concrete. This composite material does not contain rough gravel as filling, but only fine gravel of the µm size or mm maximum.

Strictly speaking, the material is not a concrete as it doesn't incorporate rough gravel but it called concrete in most of papers.

There are different ECC varieties which have different purposes [1]:

- Self-Consolidating ECC,
- High-Early-Strength ECC (HES-ECC),
- Lightweight ECC (LW-ECC),
- Green ECC (G-ECC) – is used to a large extend by product industrial waste (fly ash, blast furnace slag),
- Self-healing ECC (SH-ECC) – used especially transport engineering for proper of roads, for example.

The ECC material mixture which is discussed in this paper was based on the M45 mixture proposed by Li [2, 3, 4]. The M45 mix design was modified and the actual composition is shown in the Table 1. The original ratios of the M45 mixture components are: cement (1.0), fly ash (1.2), fine silica sand (0.8), water (0.58), high performance concrete superplasticizer admixture (0.013) and fiber components (2 %).

Table 1. ECC mix design proportions by weight

Ingredient	Cement	Cement	Fine silica sand	Water	Superplasticizer admixture	Fiber
Ratio	1.0	1.2	0.8	0.52	0.033	2 %
Weight (kg)	583	700	467	298	19	18,2

Ingredients

The portland cement (with the strength of 42.5 MPa) with high initial strength was used as a binding material according to the EN 197-1 as a CEM I 42,5 R material. The fine gravel component consists of very fine silica sand of the finest grain (0.1 – 0.3 mm). The chemical composition of the silica sand is: SiO_2 99.57 %, Al_2O_2 0.116 %, Fe_2O_3 0.053 %, TiO_2 0.113 %, CaO 0.002 % a K_2O 0.003 %.

The additive component consists of a fly ash from the local coal power plant Dětmarovice (it was used as a fly ash according to the ČSN EN 450-1 – an additive of second kind – pozzolana or latent hydraulic additives). The fly ash is produced during interaction generating of electricity and heat as by-product.

The polypropylene multifilament fiber KrampeFibrin PM 12/32 (fibres are 12 mm long, with a diameter 32 μm and a density 900 kg/m^3) is used as a reinforcing element. The PP fiber was selected because of the lack of PVA fiber in the Czech Republic.

The fluidity of the mix ensured with a fluid high performance concrete superplasticizer Glenium 110, which does not contain chlorides and which follows the ASTM C494 for the A and the F types. The superplasticizer Glenium is an additive based on modified polycarboxylic ether acid.

Costs of ingredients

The price of the Green ECC (G-ECC) ingredients was analysed. The price in Czech crowns (Kč) is given in the Table 2. The prices are calculated for production of 1 m^3 of fresh mixture. The given price includes local taxes (21 % of basic price).

Table 2. Prices of ingredients per 1 m^{3}of the G-ECC fresh mix

Ingredients	Cement	Fly ash	Fine silica sand	Water	Admixture superplasticizer	PP fiber
Weight (kg)	583	700	467	298	19	18.2
Price per weight (Kč/kg)	3.6	0.15	3.0	0.035	45	151.25
Ingredient price (Kč)	2098.8	105	1401	11	855	2752.75
Total price	7224 Kč per 1 m^3 of G-ECC fresh mix					

Production of fresh mix of G-ECC material

The production of G-ECC composite requires a strict control of the technological procedure. The stir procedure must be properly controlled in order to prevent creation of larger pieces of poorly homogenized material [5]. For this reason a mixing machine with internal volume of 100 liters has been used.

Fig. 1: Preparation of ingredients

The production procedure followed the Li's recommendations [1]: The first step is a preparation of components in the proper volumes according to Table 1. The sand is the first component which has to be added to the stirring machine. Then a 95 % of water and a full volume of superplasticizer should be added. Then the stirring machine should run on high speed for two minutes. The next step is an insertion of fly ash and cement and the rest of water. Then the stirring machine should run on a high speed for five minutes. The last additions should be the PP fibers. Then the machine runs on a high speed for further five minutes.

Fig. 2: Addition of the reinforcing PP fibers

The slump flow test of the fresh mixture resulted in the diameter of 640 mm (see Fig. 3). It means that the mixture can be classified as a mixture of the F4 class (that is a mixture with resulting diameter 550 ± 100 mm and with density of 2000 ± 50 kg/m^3).

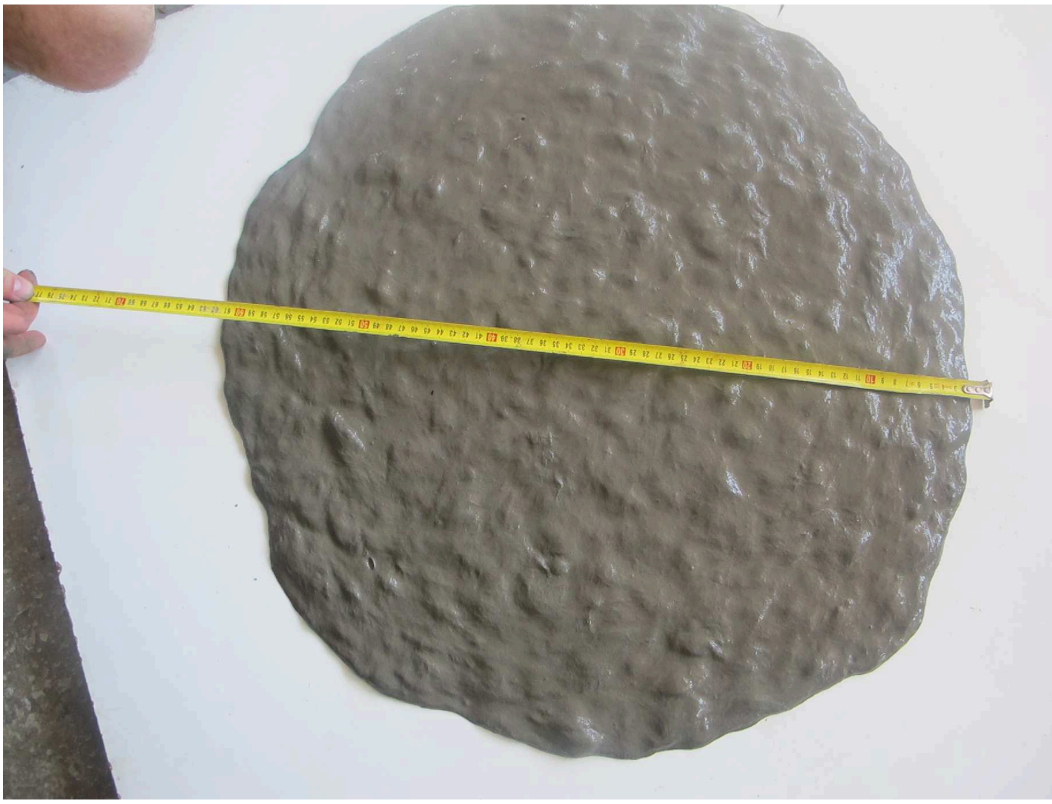

Fig. 3: The slump flow test the consistency of the G-ECC

The ECC material should have a strain-hardening behaviour during crack propagation. It means that after a creation of first cracks does not mean a decrease of bearing capacity, it should show a hardening behaviour, instead. During continuing increase of load size the material should reach the peak stress and the decreasing of bearing capacity should occur.

Fig. 4: ECC specimen after repeated compressive strength test

It can be observed from Fig. 4 that the developer ECC composite has the proposed behaviour. The strain-hardening can be identified (the initial jump in the bearing capacity around 2.0 mm is not the strain-hardening effect [6], it is rather an effect of testing device behaviour) but an initiation of cracks is hard to identify from the load-displacement curve. The peak load is reached for the deformation of about 5 mm and then decreasing of bearing capacity (the softening of material) can be identified. It is obvious that initial behaviour of the material is very similar to the normal strength concrete (NSC). In the later phases of loading it behaves more as a metal. The first crack were observed for the strain of a size $\varepsilon \approx 0.01$ %. For the strain of size $\varepsilon \approx 1$ % it was found that the crack size is about 60 μm. Further cracks are development during further increase of the deformations but the widths of microcracks remain to be near constant with size about 60 μm [1]. A failure should occur after a crack plane is developer by merging of individual cracks.

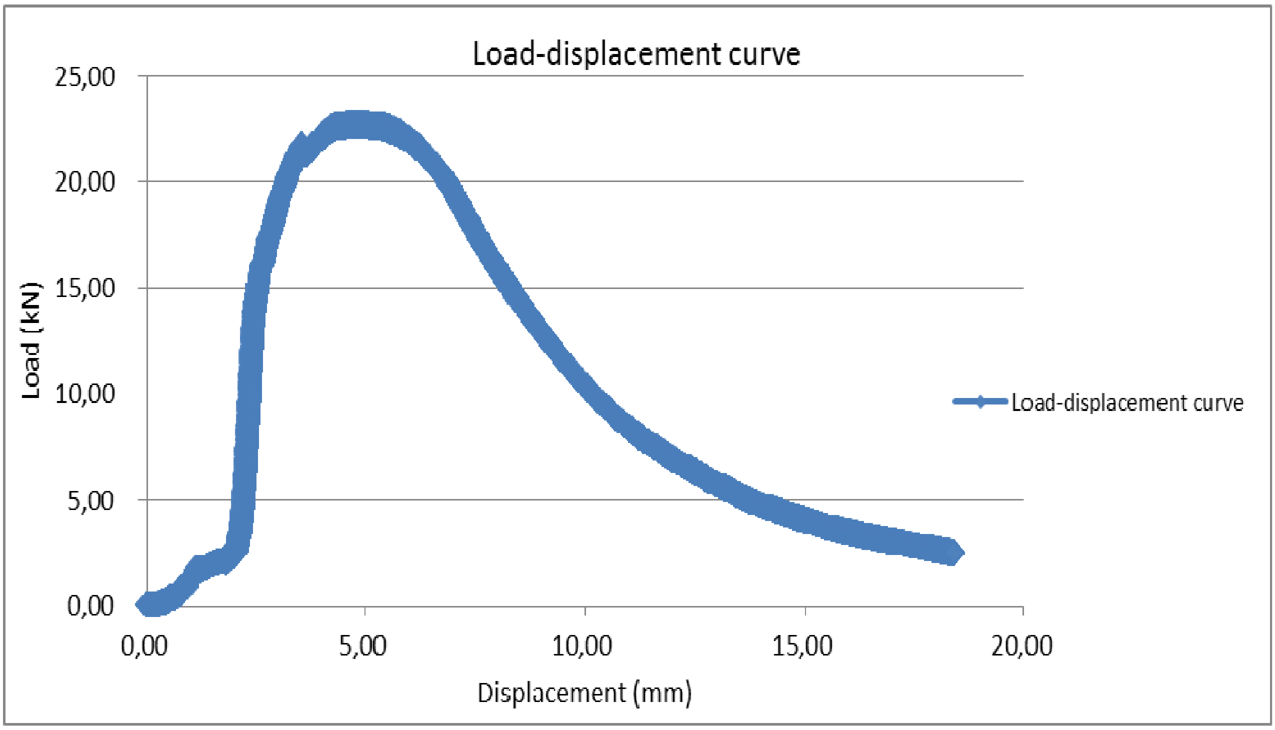

Fig. 5: Load-displacement relation of the G-ECC material

The fibers in the ECC material should interact with the matrix of this composite material. It limits reaction of the microcracks and it also has an important influence on a residual strength of the material. The total failure can occur only when bearing capacity of the fibers is fully exhausted.

The main mechanical properties of the developed G-ECC material are given in Table 3.

Table 3. Main mechanical properties of the G-ECC

Compressive Strength (MPa)	Tensile Strength (MPa)	Ultimate Tensile Strain (%)	Young's Modulus (GPa)	Density (kg.m^{-3})
72	8.9	3.0	27.2	1990

Conclusions

It can be concluded than the selected mixture was correctly selected and the material was flawlessly prepared (see Fig. 4 and Table 3 for obtained material behaviour and main properties). The compressive strength is in relation with upper limit of the interval 20-95 MPa which is given by Li [1]. The obtained ultimate tensile strain is in the middle of the interval given by Li (1-8 %).

The further works will be focused on a development on a more environmentally friendly composite. The portion of the cement will be partially replaced by the fly ashes and the optimal ratio will be searched. There will be also works on addition of other components to the mixture in order to save the most expensive ingredients.

An another aim of the development team is a development of a material with a better ration between the ultimate strain and the tensile strength.

Acknowledgement

The works were supported from funds for conceptual development of research, development and innovations for 2014 at the VSB-TU of Ostrava which were obtained from the Ministry of education, youths and sports of the Czech Republic.

References

[1] LI, Victor C. *Concrete Construction Engineering Handbook*. Second Edition. Rutgers University, Piscataway, New Jersey, USA. Boca Raton : CRC Press, 2008. Engineered Cementitious Composite (ECC): Material, Structural, and Durability Performance, s. 1024-1069. ISBN 9780849374920.

[2] LI, Victor C., et al. Development of green ECC for sustainable infrastructure systems. In Proceedings of the International Workshop on Sustainable Development and Concrete Technology, May 20–21, Beijing, China, Wang, K., Ed., pp. 181–192.

[3] LI, Victor C. 2006. Integrated structures and materials design. RILEM J. Mater. Struct., 40(4), 387–396.

[4] JAŠEK, Marek. *Posouzení nových materiálů a technologií pro zesilování zděných konstrukcí*. Ostrava: Vysoká škola báňská – Technická univerzita Ostrava, 2011. 187 s. Disertační práce. Vysoká škola báňská – Technická univerzita Ostrava, Fakulta stavební.

[5] Kajima Technical Research Institute. 2006. Mixing Manual of ECC Dry-Mix for Casting, KaTRI, Japan. 2006.

[6] KOLÍSKO, Jiří. *Vliv krátkých všesměrně rozptýlených polypropylénových mikro a makrovláken na vlastnosti cementových malt a betonů*. Praha : ČVUT, 2008. 24 s., ISBN 978-80-01-04072-0.

Advanced Materials Research Vol. 1020 (2014) pp 9-14
© (2014) Trans Tech Publications, Switzerland
doi:10.4028/www.scientific.net/AMR.1020.9

Applications of titanium sheets in modern building construction

ADAMUS Janina

Czestochowa University of Technology, Dabrowskiego 69, 42-201 Czestochowa, Poland

email: janina.adamus@gmail.com

Keywords: civil engineering; titanium; sheet; sheet-metal forming.

Abstract. Titanium is most likely to play more important role in future civil applications. Its excellent properties such as: low density, high mechanical strength and good corrosion resistance give it some advantages and open the way for new applications both in modern technology and civil engineering. In many ways (e.g. specific strength, corrosion resistance) titanium, especially its alloys outstrip structural materials such as steel and aluminium alloys. The article discusses titanium properties, which are important in civil engineering such as: low density, resistance to sea water and salty atmospheres, low coefficient of thermal expansion and excellent aesthetic qualities. Although its use in civil application is still limited it is expected that a demand for titanium building materials will steadily grow in future. The characteristic titanium applications in the worldwide civil engineering are presented. It is highlighted that over a long span of 20 or more years titanium tends to be cheaper than other materials in terms of life-cycle costs. Furthermore, the article investigates the difficulties and opportunities associated with titanium forming. Some technological problems (e.g. low formability, high susceptibility to galling and high spring-back) occurring in the sheet-titanium forming processes are discussed.

Introduction

In the world there is a tendency to replace traditional metals, mainly steel, with light materials having good corrosion resistance. Titanium satisfy these requirements. Until recently, it was considered as a strategic material used for military purposes, especially in aerospace, aviation and maritime industries [1-5], as well as in the industries where it was absolutely necessary e.g. in the chemical industry. Currently, titanium materials are increasingly used in civil applications, such as automotive industry and medicine [6-8]. An interest in the use of titanium in the civil engineering grows due to excellent corrosion resistance, low specific gravity, high strength and low thermal conductivity. Although the use of titanium is limited owing to high production costs and difficulties in its processing [9-11], it is likely that along with the development of new technologies [12-17] titanium use will increase.

Titanium and its alloys

Both titanium and its alloys are used in modern technologies. According to ASTM B265 five grades of commercially pure titanium: Gr 1÷4 and Gr 7 are produced. Depending on production technology each grade has a different degree of impurities. The higher impurities content corresponds to higher mechanical strength and lower material plasticity. Gr 1 has the lowest impurities content. Yield strength changes from 170 MPa for Gr 1 to 480 MPa for Gr 4, and tensile strength changes from 240 to 740 MPa, respectively. Alloying additives increase the tensile strength over 1200 MPa [7, 18-20]. Titanium alloys are classified into three categories: α, $\alpha+\beta$ and β or near-beta alloys. α titanium alloys, due to high heat strength, are used for parts working at elevated temperature and because they do not exhibit a ductile-to-brittle transition they are also suitable for cryogenic applications. Ti5Al2,5Sn and Ti5Al2 alloys are the most often applied alpha titanium alloys. At ambient temperature α and $\alpha+\beta$ titanium alloys can be plastically deformed to a small extent since they have high yield-to-tensile strength ratio (above 90%). Just above 500°C the ratio improves, so these alloys are usually semi-hot or hot formed. However, this entails the need to solve the problem of high susceptibility to gas absorption (oxygen, nitrogen, hydrogen), which causes structural changes and reduces titanium strength. Ti6Al4V alloy is the most commonly used alloy. After heat treatment its tensile strength reaches 1170 MPa. β titanium alloys have good formability, even using cold working. They can be hardened by heat treatment. Annealed Ti13V11Cr3Al alloy has the tensile strength of 930 MPa but after heat treatment its tensile strength can reach the value of 1750 MPa that makes it the highest strength metal among all known structural materials [1,21,22].

Advantages and disadvantages of titanium

Titanium is a metal with low density being about 60% that of steel. It can be alloyed with Fe, Al, V, Mo and other elements, to produce strong lightweight alloys that have the most favourable specific strength (material strength-to-weight ratio) of any structural metals in the temperature range up to 600°C. Additionally, low Young's modulus - from 80 to 110 GPa [23], which is approximately one half that of steels, makes it an attractive material for springs. That in conjunction with the high strength and low density could perfectly result in a weight savings of about 70% of that of a steel spring.

Titanium is an active metal but because of a passive film of titanium oxide, it exhibits extremely high corrosion resistance to many environments, including sea water. An increase in corrosion resistance is obtained thanks to anodic oxidation. Another advantage of this process is the ability to achieve visually attractive colour tones of high saturation. The oxidized film is colourless and transparent and has a very strong refraction ratio. So the colour effect results from interference of refracted and reflected back light hitting this transparent film. A wide range of colours can be achieved by using a suitable film thickness [24].

Additionally, titanium is environmentally friendly, i.e. it is 100% recyclable.

Despite so many advantages titanium production and processing pose considerable difficulties due to high susceptibility to gas absorption, low plasticity and poor tribological properties.

Titanium advantageous with respect to civil engineering. Good corrosion resistance and low specific gravity are the most important for civil engineering. Due to growing environmental pollution the traditional structural materials cannot meet requirements of corrosion resistance. Until recently, during long-term exposure to weather conditions copper underwent passivation - green patina was covering external layers of copper parts. Currently, as a result of increasing air pollution by SO_2, the patina includes basic copper sulphate $(CuOH)_2SO_4$. This prevents patina from providing further protection against corrosion. Durability of copper roofs dropped from around 80 to 20 years, so alternative materials having better corrosion resistance are sought. Titanium seems to be such a material. Manufacturers guarantee its corrosion resistance in the period of 50÷100 years. Thus the interest in the use of titanium for roofing, building interior and exterior, facades grows. Titanium structures are light and aesthetics. Titanium is extremely practical due to structure durability and maintenance costs. It is resistant to the increasing pollution in urban areas, acid rains, marine environment, volcanic ash and does not degrade in response to ultraviolet radiation. Titanium does not require additional corrosion protection, while other metals erode and corrode releasing metal ions that contaminate groundwater. Although initially material costs are several times higher than conventional metals, in the long-term maintenance costs are much lower. This is especially true in the case of structures exposed to highly corrosive environments, i.e. in coastal and industrial areas.

A low coefficient of linear thermal expansion allows titanium components to work together with ceramics, glass and concrete without danger of distortion or fatigue due to changing heat loads. The combination of high tensile strength and low Young's modulus with low density makes titanium alloys resistant to sudden and variable loads. This means that titanium alloys used in architectural structures, especially in areas prone to earthquakes and violent tectonic movements will be more flexible than other structural metals. Fig. 1 shows the density and linear coefficient of thermal expansion of the selected materials.

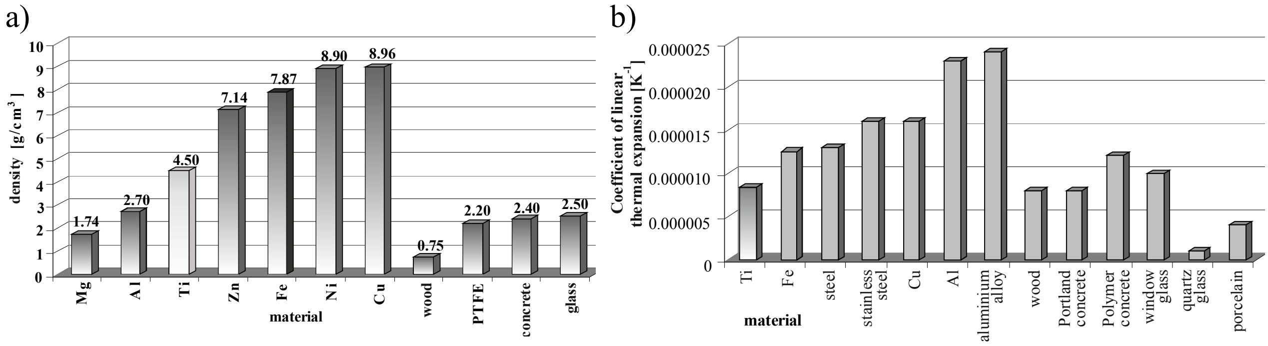

Fig. 1. Titanium versus other structural materials: a) density, b) coefficient of heat expansion [21,22, advertising materials of JFE Steel Corporation]

Large roofs made of typical thin sheets require a seam system to compensate for thermal expansion and contraction. Titanium roofs can be made from single panels, since the thermal stress is lower than that of stainless steels, copper or aluminium. The amount of thermal expansion is a function of panel's length, magnitude of temperature change, and coefficient of thermal expansion. Greater lengths of titanium roofing sheets reduce installation cost. Low thermal conductivity, 21.6 $Wm^{-1}K^{-1}$, which is ten times lower than aluminium one, also means that titanium can be used in construction. Titanium, having a melting point of 1668°C, is classified as a non-combustible material, suitable for roofs and facades of buildings.

Titanium applications in civil engineering

Generally, titanium applications divide into three groups, which requires: light metals with high mechanical strength, corrosion-resistant materials or specific properties (e.g. biocompability).

Although in the West titanium appears as a relatively new architectural material in the East, especially in Japan - in a highly industrialized environment with a strong influence of sea, there are hundreds of buildings made of titanium. The first titanium applications in Japanese architecture date from the early seventies of 20th century. These were mainly roofs. Some examples are shown in Fig. 2. The Fukuoka Dome from 1993 is a noteworthy architecture example (Fig. 2a). It is a modern sport centre with a retractable roof having a diameter of 222 m and field area of 13,500 m^2. The roof is made from three fan-shaped panels, which are covered with 3-millimeter thick titanium sheets. Fig. 2b shows the glossy blue roof of the Kyushu National Museum, made of anodised titanium sheets. During renovation of ancient roofs it is necessary to solve the problem of maintaining the original appearance of objects, such as temples or shrines. For this purpose, titanium sheet surface is treated (e.g. by using different kinds of alumina blasting deliberately varied to obtain the diverse degree of luster of titanium) to give it a texture similar to smoked tiles (Fig. 2c).

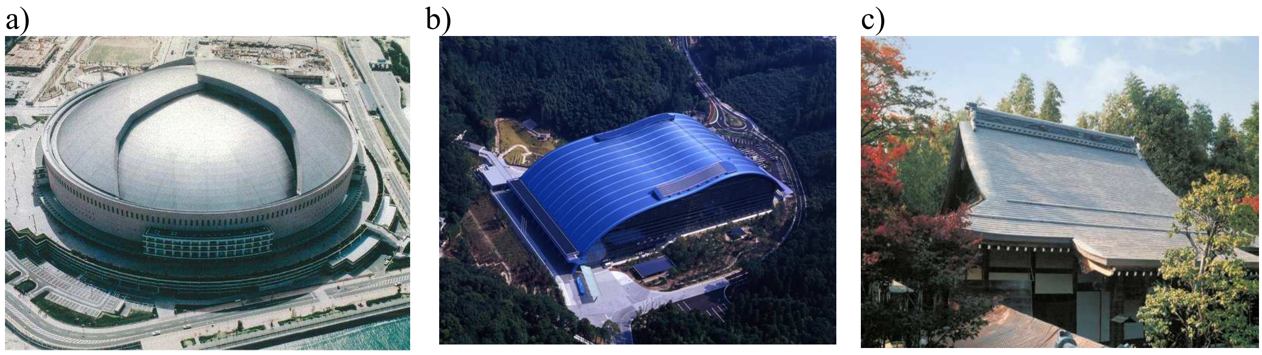

Fig. 2. Examples of titanium applications in Japaneese architecture: a) Fukuoka Dome, b) Kyushu National Museum, c) Koetsu-Ji shrine in Kyoto

In European titanium constructions, the Spanish museum of modern and contemporary art - Guggenheim Museum Bilbao is particularly noteworthy, (Fig. 3a). It was designed by Canadian-

American architect Frank Gehry. 32,000 m^2 of commercially pure titanium sheets – Gr 1 with different textures, from matte to smooth, and with thickness of 0.3-0.4 mm were used for construction of this building. Titanium sheets were also used for renovation of the Van Gogh museum (Fig. 3b) and for protection of the Scheepvaart Museum in Amsterdam against the damaging effects of light, temperature and moisture (Fig. 3c). A large part of modern titanium architectural structures are monuments (e.g. the Monument to the Conquerors of Space erected in Moscow in 1964, a 107-meter height obelisk depicts a contrail of the starting rocket. It is covered with titanium sheets).

a) b) c)

Fig. 3. Examples of titanium applications in European architecture: a) Guggenheim Museum in Bilbao, b) Van Gogh Museum in Amsterdam, c) Scheepvaart Museum in Amsterdam

Metal structures have been an alternative to wooden structures for a long time. The use of titanium for the frames of various types of buildings additionally increases the strength of the buildings, especially resistance to earthquakes. Architects increasingly prefer to apply titanium because it allows for implementation of challenging solutions that are impossible using traditional materials. They apply both commercially pure titanium and titanium alloys. Potentially titanium honeycomb panels will also find application in civil engineering [25], which would allow for a substantial reduction in structure weight. For example, sandwich panels weighing 4.5 kg have the same stiffness as five times thicker single titanium sheet that is five times more heavier. Such panels consist of two titanium sheets with a special honeycomb texture. These structures are produced using the hydraulic forming process, which allows for avoiding creation of titanium protrusions on the tool surfaces, that make conventional forming impossible [26].

In recent years, titanium application to bridges and coastal structures also grows. Titanium-clad steel sheets, that are used to protect floating steel structures at their splash zone, are one of the most interesting applications. For this purpose, steel sheets are clad with thin titanium sheets during rolling through the intermediary of copper [27]. For example, 4-mm thick steel sheets clad with 1-mm thick titanium sheets were used for Tokyo Bay Highway Bridge.

Comparison between Gr 2 and Gr 5 formability

Two grades of titanium sheets: commercially pure titanium - Gr 2 and titanium alloy Gr 5 were tested. The microstructure of Gr 2 is composed of recrystallized α grains containing lenticular twins while Gr 5 microstructure contains a fine-grained globular α phase separated by the β phase precipitated along the grain boundaries (Fig. 5a,b). The Erichsen cupping test was employed to evaluate formability of titanium sheets. The test consists in forming an indentation by pressing a spherical punch against a test piece clamped between a blank-holder and a die, until a through crack appears. The test showed a significant difference in ductility of the analysed sheets (Fig. 5c,d). Depth of the bulge for Gr 2 sheet was 12 mm, while for Gr 5 sheet was only 3 mm. It means that only Gr 2 sheet can be easily formed using classical forming tools (die, punch and blank-holder) at ambient temperature. Additionally, two indicators of material formability were defined for Gr 2 sheet: limiting drawing ratio LDR=0.43 and normal anisotropy coefficient R=4.5. One of the conditions required for sheet-metal forming is that R-value is greater than 1.0. Such tests were not performed for Gr 5 sheet due to the very low formability at ambient temperature, as it can be clearly seen in Fig. 5c and d.

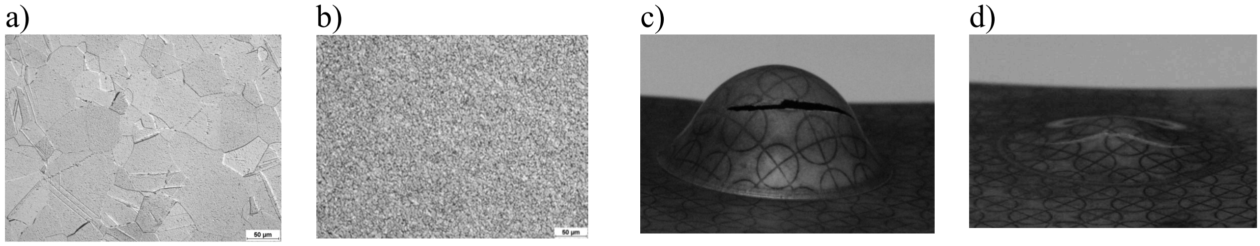

Fig. 5. Microstructure and Erichsen cupping test results: a, c) Gr 2; b, d) Gr 5 [10]

The basic mechanical properties were determined in an uniaxial tensile test. The test results are presented in Table 1.

Table 1. Mechanical and technological parameters of the tested sheets

Material	Yield point R_e [MPa]	Tensile strength R_m [MPa]	Elongation A_{10} [%]	Strain hardening exponent n [-]	Material constant K [MPa]
Gr 2	397	501	29	0.15	753
Gr 5	1009	1032	10	0.04	1256

Summary

Analysis of the technical literature and experimental research indicate that sheets of commercially pure titanium, especially Gr 1 and Gr 2 have a relatively good formability, and such sheets are mainly used for construction of roofs and facades.

Titanium and its alloys have been appreciated for years in aerospace, aviation and military applications. Currently they are increasingly used in civil applications, including civil engineering. They allow for reduction in the structure weight, while maintaining its previous strength. At the same time titanium ensures the long-term corrosion resistance. High expenditures at construction stage become justifiable taking into account low cost of maintenance.

Although the price of titanium production and its processing is several times higher compared to the price of stainless steel or aluminium, titanium products do not require expensive anti-corrosion protection. This makes titanium an attractive and competitive material in the field of civil engineering.

References

[1] R.R. Boyer, An overview on the use of titanium in the aerospace industry, Mat. Sci. Eng. A213 (1996) 103-114.

[2] H. Fujii, K. Takahashi, Y. Yamashita, Application of titanium and its alloys for automobile parts, Nippon Steel Technical Report No 88 July 2003.

[3] I.V. Gorynin, Titanium alloys for marine application, Mat. Sci. Eng. A263 (1999) 112-116.

[4] C.T.F. Ross, A conceptual design of an underwater missile launcher, Ocean Eng. 32 (2005) 85-99.

[5] C.T.F. Ross, A conceptual design of an underwater vehicle, Ocean Eng. 33 (2006) 2087-2104.

[6] C. Cui, B.M. Hu, L. Zhao, S. Liu, Titanium alloy production technology, market prospect and industry development, Mater. Design 32 (2011) 1684-1691.

[7] Y. Kosaka, S. P. Fox, K. Faller, Newly developed titanium alloy sheets for the exhausted systems of motorcycles and automobiles. JOM, November 56/11 (2004) 32-34.

[8] V. Jablokov, B. Drummond, N. Hoskison, Processing and properties of Allvac Ti-38-644 for titanium automotive suspension springs. Aluminum, ed. by Subodh K.Das TMS, 2004.

[9] J. Adamus, P. Lacki, Possibility of the increase in titanium sheets' drawability. Key Eng. Mat. 549 (2013) 31-38.

[10] J. Adamus, P. Lacki, M. Motyka, K. Kubiak, Investigation of sheet-titanium drawability. Ti 2011 - Proceedings of the 12th World Conference on Titanium 1 (2012) 337-341.

[11] P. Lacki, J. Adamus, W. Więckowski, J. Winowiecka, Evaluation of drawability of titanium welded sheets. Arch. Metall. Mater. 58 (1) (2013) 139-143.

[12] J. Adamus, P. Lacki, Forming of the Titanium Elements by Bending, Comp. Mater. Sci. 50/4 (2011) 1305-1309.

[13] J. Adamus, P. Lacki, Investigation of sheet-titanium forming with flexible tool - experiment and simulation, Arch. Metall. Mater. 57/4 (2012) 1247-1252.

[14] J. Adamus, P. Lacki, W. Więckowski, Numerical simulation of the fine blanking process of sheet titanium, Arch. Metall. Mater. 56 (2) (2011) 431-438.

[15] P. Lacki, Simulation of sheet-titanium forming of welded blanks, Proceedings of the 12th International Conference on Computational Plasticity - Fundamentals and Applications, COMPLAS'2013, Barcelona – Spain, (2013) 854-861.

[16] P. Lacki, J. Adamus, M. Motyka, J. Sieniawski, Theoretical and experimental analysis of a ring compression test for Ti-6Al-4V titanium alloy, Ti 2011 - Proceedings of the 12th World Conference on Titanium 1 (2012) 333-336.

[17] P. Lacki, K. Adamus, Numerical simulation of welding thin titanium sheets, Key Eng. Mat. 549 (2013) 407-414.

[18] A. Bylica, J. Sieniawski, Titanium and its alloys (in Polish: Tytan i jego stopy), PWN, Warszawa-Poland, 1985.

[19] K. Kutzsche, W. Hennig, Umformfestigkeit von Titan. Neue Hütte 35 (1990) 149-15.

[20] R. Melechov, K. Tubielewicz, W. Błaszczuk, Titanium and its alloys (in Polish: Tytan i jego stopy), Wyd. Politechniki Częstochowskiej, Częstochowa-Poland (2004).

[21] R. Boyer, G. Welsch, E. W. Collings: Materials properties handbook: Titanium alloys. ASM International, Materials Park, OH (1994).

[22] J. R. Davis ed.: Metals Handbook, vol. 2 - Properties and Selection: Nonferrous Alloys and Special-Purpose Materials. ASM International 10th Ed., (1990).

[23] T. Ozaki, H. Matsumoto, S. Watanabe, S. Hanada, Beta Ti Alloys with Low Young's Modulus, Mater. Trans. 45/8 (2004) 2776-2779.

[24] T. Wierzchoń, E. Czarnowska, D. Krupa, Surface engineering in production of titanium biomaterials (in Polish: Inżynieria powierzchni w wytwarzaniu biomateriałów tytanowych), Oficyna Wydawnicza Politechniki Warszawskiej, Warszawa-Poland (2004) (in Polish).

[25] W. Han, K. Zhang, G. Wang, Superplastic forming and diffusion bonding for honeycomb structure of Ti6Al4V alloy. J. Mater. Process. Tech. 183 (2007) 450-454.

[26] J. Adamus, Stamping of the Titanium Sheets. Key Eng. Mat. 410-411(2009) 279-288.

[27] S. Nakamura, K. Homma, Durability of Titanium-Clad Steel Plates used as an Anti-Corrosion System, Structural Engineering International, 10/4 (2000) 262-265.

Advanced Materials Research Vol. 1020 (2014) pp 15-20

doi:10.4028/www.scientific.net/AMR.1020.15

Galvanised sheets as building material

ADAMUS Janina[1a], GIERZYŃSKA-DOLNA Monika[1b], GORECKI Wilhelm[2c] and LACKI Piotr[1d*]

[1] Czestochowa University of Technology, Dabrowskiego 69, 42-201 Czestochowa, Poland

[2] Silesian College of Economics and Administration in Bytom, A. Frycza-Modrzewskiego 12, 41-907 Bytom-Szombierki, Poland

[a] janina.adamus@gmail.com, [b] monika.gierzynska.dolna@gmail.com, [c] wilgo@vp.pl, [d] piotr@lacki.com.pl, * corresponding author

Keywords: civil engineering; corrosion; galvanised sheet; sheet-metal forming.

Abstract. Civil engineering uses steel as one of the basic structural materials. Sheets play an important role among the steel products. Although steel sheets are relatively cheap and have good mechanical and technological properties, low resistance against corrosion poses a fundamental weakness. A solution to this problem is the use of galvanised or organic-coated steel sheets. Galvanising can be carried out by hot dipping (single structural parts) or continuous galvanising: electrolytic and hot-dip galvanising (sheets and strips or long products, such as: wires or pipes).

In the paper steel sheets used in the civil engineering as structural parts or wall and roof cladding are discussed. A special attention is paid to corrosion resistance of the steel sheets. Some results of corrosion tests is presented. The influence of the galvanising technology and the relationship between the degree of material deformation and susceptibility to corrosion are given. Coating thickness and kind of the applied galvanising technology is pointed as the key factors affecting the corrosion resistance of galvanised sheets. It is highlighted that during the forming process of galvanised sheets (bending, sheet-metal forming) the zinc coating deforms more than the steel base, so its thickness decreases, and therefore the corrosion resistance of the final product decreases, too.

Introduction

Civil engineering uses steel as one of the basic structural materials. It results from the fact that steel has good mechanical and technological properties, is cheap and suitable for recycling. The modern structural steel surpasses its main rivals, such as aluminium, plastics or composites in the common use. Unfortunately, steel has a fundamental disadvantage – a poor corrosion resistance. A solution to this problem is the use both galvanised and organic-coated steel sheets [1 5]. Galvanising successfully protects steel products against corrosion. There are two basic galvanising methods [2]: hot dipping, used for single structural parts, and continuous galvanising (electrolytic and hot-dip galvanising, used for flat products, such as: sheets and strips, or long products, such as: wires and pipes).

In [6,7] an analyse of conventional hot-dip galvanised pure Zn, galvannealed and Zn-Al alloy coatings on steel to explain mechanism of corrosion resistance is given. A discussion on corrosion behaviour of rare earth ion-implanted hot-dip galvanised steel is presented in [8,9]. Hadi and Li [10] investigates a number of high strength concrete columns that are externally reinforced with galvanised steel straps subjected to concentric and eccentric loading. The experimental results show that external reinforcement can enhance the properties of high strength concrete columns.

Steel sheets in civil engineering

Sheets are the basic steel products. Hot-dip galvanised sheets [4] and organic-coated steel sheets [5] are mainly used in the civil engineering. The sheet production develops gradually [2] from hot-dip galvanising of single sheets to continuous hot-dip galvanising (the Sendzimir galvanising process). In order to improve paintability and weldability of galvanised sheets galvannealing was introduced in the 50s of the 20th century. It combines process of galvanizing and annealing to produce specialized steel sheets characterising by a greyish matte finish. Galvannealed coat does not flake off the base when formed, stamped and bent. Nowadays, this method is extensively used in the automotive industry (car body sheets). Moreover, galvanised sheets with addition of aluminium: Galfan (5% Al-Zn coated steel) and Galvalume (55% Al-Zn coated steel), and galvanised sheets for coil coating (minimized spangle, spangle-free sheets) are produced. In the civil industry hot-dip galvanised sheets, Galfan and Galvalume, as also organic coated sheets are mainly used. Thanks to strong anti-corrosion properties Galfan and Galvalume are suitable for roofing and siding.

The sheets are cold-formed in roll forming machines (corrugated, trapezoidal and roofing sheets) or they are used as cladding panels (with a thick insulation layer). The sheets are also used as starting material for manufacturing large welded sections, specially designed for industrial buildings. At present the following steel sheets are produced in Poland:

- corrugated sheets (slowly dying production),
- trapezoidal sheets, mainly organic-coated sheets (6 roll forming lines in the steel industry and several roll forming lines in other industrial plants – mainly in the private sector). The height of produced trapezoidal sheets: T12÷T160 mm,
- tile-type roofing sheets (one line in the steel industry and several profiling lines in other industrial plants – mainly in the private sector),
- welded large sections with a straight or wavy web,
- Z-type sections for industrial buildings,
- cladding panels.

At the moment Galfan and Galvalume galvanised sheets are not produced in Poland.

Recently the building industry was dominated by administrative- and service-buildings of a light metal frame construction, with metal walls and roofs. Both plain steel sheets and roll-formed (corrugated or trapezoidal) sheets are used for roofing and cladding panels. In the case where insulation properties of the structural material are irrelevant, only blank sheets are used, while for the case where good thermal insulation is required - panels, consisting of an insulating core coated on both sides with profiled sheets, are used. In the housing industry, steel tile-type roofing sheets are the latest generation of roofing materials, combining the traditional appearance with a modern technology. When using this type of sheets, a strong supporting structure is not required. Additionally, the colour variety of anti-corrosion coatings provides a wide range of architectural options. In Fig. 1 some examples of galvanised steel sheets used in the civil industry are shown.

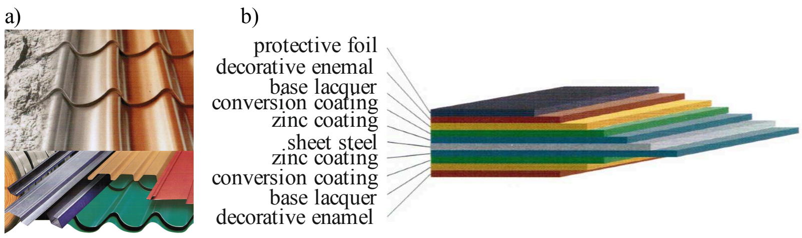

Fig. 1: Steel sheets used in civil industry [11]: a) roll-formed sheets, b) organic-coated steel sheet

Galvanised steel sheets – resistance to corrosion

Zinc is more electronegative than steel so it provides effective cathodic (sacrificial) protection against corrosion. Zinc cathodic protection means that the steel core does not undergo corrosion, even if the zinc coat is locally damaged. In the surrounding areas the zinc coat is dissolving. Corrosion of the steel will occur when the zinc coat dissolves completely. It is very important in the case of galvanised sheets with sheared edges (shearing to the required size).

In 2010 the total world production of zinc, was 11 million tons, of which 47% were used for protection of steel products against corrosion [12].

Thickness of zinc coat, terms and conditions of sheet storage, and method of sheet-metal forming are the main factors affecting corrosion resistance of galvanised sheets. There is a linear relationship between the zinc coat thickness and the corrosion resistance: the thicker the zinc coat, the higher the corrosion resistance of galvanised sheets. The thickness of zinc coats ranges from 5.0 to 45 μm/side (i.e. 70÷600 g/m^2/two-sided) for hot-dip galvanised sheets, and from 0.3 to 3.0 μm/side for electrolytic galvanised sheets [2]. The zinc coat is a durable and relatively inexpensive protective coat, but it also has a disadvantage, which is unknown to many users. Due to improper storage of galvanised sheets, as a result of moisture and absence of air, "white corrosion" appears on the sheet surface. Such corrosion rapidly destroys the zinc coat, accelerates corrosion of the steel core and finally results in an inability to further sheet-metal processing. In order to avoid this problem, gathering of sheets into piles takes place at a specified temperature and humidity in the finishing department of the galvanising plant. Sometimes manufacturers of galvanised sheets give to customers a special instruction for correct handling with the sheets during storage and use.

Galvanised sheets are often cold-formed in the roll forming machines or bending and stamping presses. During these operations, both the steel core and the zinc coat are deformed. As the yield stress of zinc (R_e=30 MPa) and steel (R_e=180 MPa) differs fundamentally, the soft zinc coat deforms more than the hard steel core [13, 14]. As a result of the forming a significant reduction in thickness of the zinc coat occurs. It reduces the corrosion resistance of the galvanised products.

Goal and scope of experiments

The study aims at determination of the galvanising technology influence on corrosion resistance and the relationship between the deformation value and susceptibility to corrosion [15,16].

Uncoated low-carbon steel sheets, electrolytic galvanised low-carbon steel sheets, hot-dip galvanised sheets, hot-dip galvanised and skin-passed sheets, and galvannealed sheets were tested. The first batch of the samples was taken from the strips 20x250mm in size, which had undergone the tensile test with the following degrees of deformation: ε_1 = 0%, 10%, 20%. The samples with dimensions of 65x65mm, which had undergone the Erichsen cupping test to the height of 6.0 and 8.5 mm comprised the second batch. The third batch of samples was subjected to bending, while the cylindrically drawn-parts with the diameter and height of 35 mm comprised the fourth batch.

The following corrosion tests were applied:

- in a salt mist chamber at an ambient temperature (20^{o}C), according to the valid standard,
- in a climatic chamber with salt mist at a temperature of 35^{o}C, according to the valid standard,
- an immersion method in a 10% solution of NH_4Cl at an ambient temperature, according to the valid standard.

The tests in the mist chamber were carried out for a period of 14 days. Due to the fact that the zinc coat on steel is an anodic coat, the degree of corrosion was determined in accordance with the valid standard, resulting in observations of the coat surface and the degree of its corrosion, expressed in [%]. In the immersion method, the K_B index, expressing the ratio of weight loss of the sample to the surface, which was subjected to corrosion, has been assumed as the criterion for the degree of metal corrosion.

$$K_B = \frac{\Delta G}{A}\left[g/mm^2\right], \tag{1}$$

where: ΔG - mass loss of the sample, A - surface, subjected to corrosion.

The study was carried out for 30 days. The samples were weighed every 3 days, after the removal of corrosion products.

Test results

Microstructures of the analysed galvanised coats are shown in Fig. 2, while the results of the corrosion test in the mist salt chamber at ambient temperature are presented in Fig, 3a.

a) b) c)

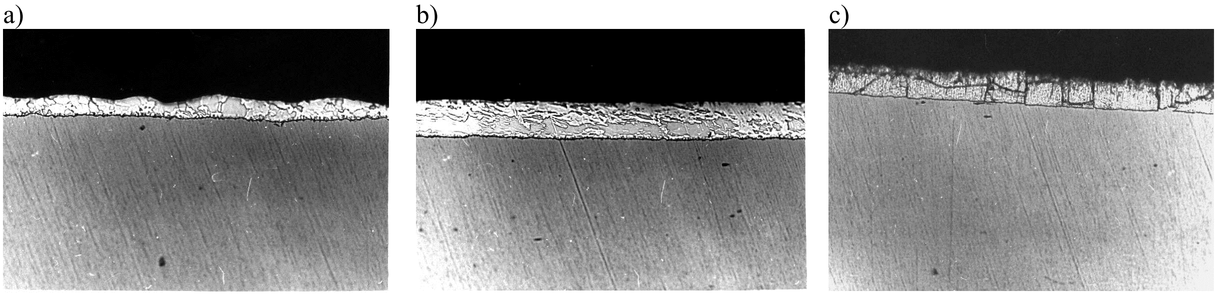

Fig. 2. Zinc coats (magnification 50x): a) electrolytic, b) hot-dip galvanised and skin-passed, c) galvannealed sheets

The carried out tests show that uncoated steel sheets corrode the earliest. The first signs of corrosion appeared on the first day of exposure. The electrolytic galvanised samples also showed a high susceptibility to corrosion. In this case, the first corrosion signs appeared on the steel base already on the 5th day of the test. Initially, it was a very slight corrosion, which then gradually grew-up. On the 8 – 9th day the corroded surface took more than 50% so the tests were interrupted on the 9th day. The hot-dip galvanised, skin-passed steel sheets showed the greatest corrosion resistance. It results from the fact that during the skin passing rolling process the zinc coat is sealed and smoothed (Fig.2b). It delays the corrosion process itself. Hot-dip galvanised steel sheet shows a little bit worse corrosion resistance. In all cases, the corrosion intensity depended on the degree of deformation. The deformed (stretched) sheets with ε=10÷20% corroded faster than the non deformed ones, which can be explained in two ways:

- a decrease in thickness of the zinc coat due to its deformation,
- the additional stresses as a result of strain hardening.

Results of the corrosion tests carried out in the climatic chamber at 35°C are shown in Fig. 3b.

a) b)

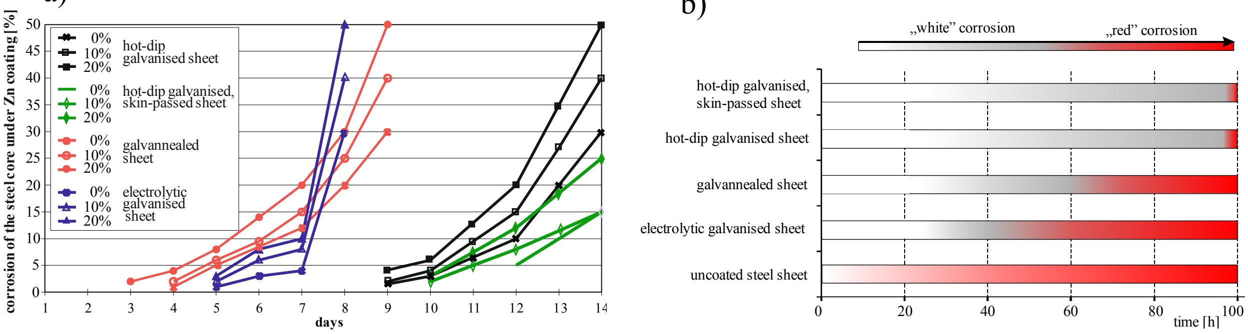

Fig. 3. Test results of corrosion resistance of steel sheets: a) in salt mist chamber at 20°C, b) in climatic chamber at 35°C, [16]

The tests were carried out for 100 hours. In the case of uncoated steel sheets the first signs of a "red" corrosion occurred after the first hour of exposure in the chamber. The galvanised steel sheet, at first covered with "white" corrosion, which increased over the time. In the case of the electrolytic galvanised sheet, the first signs of "red" corrosion appeared after 48 hours, while for the galvannealed steel sheet - after 66 hours of exposure. Hot-dip galvanised steel sheets showed the highest corrosion resistance (the first signs of a "red" rust occurred after 96 hours). For the hot-dip galvanised, skin-passed steel sheets the "red" rust appeared in the 98 hour of exposure. These test results are convergent with the results of the tests carried out in the mist salt chamber at ambient temperature. Due to the fact that the two first testing methods were based on a subjective assessment of the corrosion degree of the surface (estimated as a percentage), further tests were carried out using an immersion method, allowing a quantitative assessment of the corrosion intensity. Results of the corrosion tests carried out by immersion in a 10% NH_4Cl – solution at 20°C are illustrated in Fig. 4-5. Fig. 4a shows the results of corrosion tests for uncoated steel sheets. The study showed that the greatest intensity of corrosion occurred in the case of cylindrical drawn-parts and samples deformed in the Erichsen cupping test. The lowest intensity of corrosion occurred for the samples made of non deformed sheets and then stretched to the degree of elongation ε=10÷20%. The corrosion intensity for the bent samples was similar to the samples stretched with ε=10%. A similar regularity was also observed in the case of other tested sheets. Fig. 4b, 5a and 5b show the corrosion intensity for electrolytic galvanised sheets, hot-dip galvanised sheets and hot-dip galvanised and skin-passed sheets, respectively.

a) b)

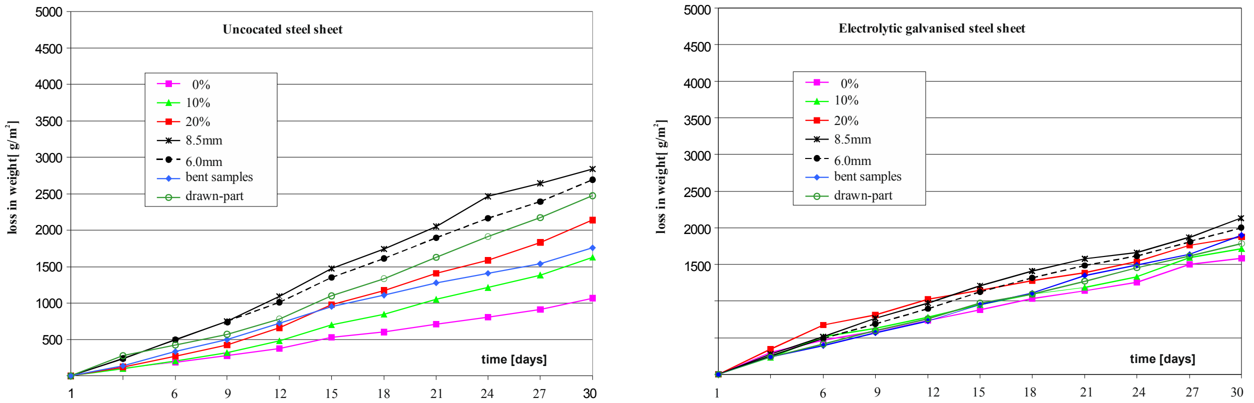

Fig. 4. Test results of corrosion resistance of: a) uncoated, b) electrolytic galvanised steel sheets [16]

a) b)

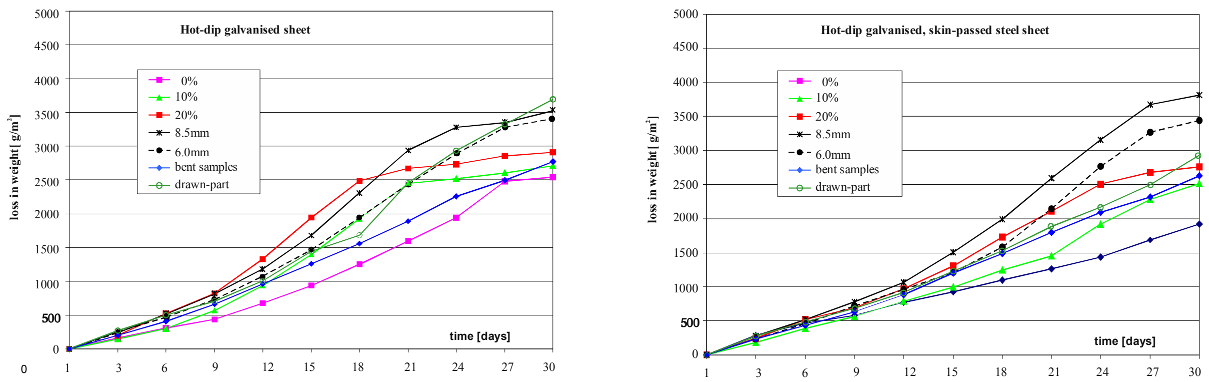

Fig 5. Test results of corrosion resistance of: a) hot-dip galvanised b) hot-dip galvanised, skin-passed steel sheets [16]

The galvannealed sheet steel showed the greatest susceptibility to corrosion. It results from the low coating density and the fact that the local galvanic microcells had been formed in the Fe-Zn alloy layer. In the immersion method the electrolytic galvanised sheet showed a quite good corrosion resistance.

Summary

Concluding it can be stated that hot-dip galvanised sheets used in the civil engineering show quite good corrosion resistance. However, galvanised sheets are a very "sensitive" product, which need to be stored under special conditions (creation of the "white" corrosion).

During the forming process of galvanised sheets (bending, sheet-metal forming) it is necessary to remember that the zinc coating deforms more than the steel base, its thickness decreases, and therefore the corrosion resistance of the final product decreases, too.

References

[1] J. Adamus, Forming drawn-parts from coated sheets (in Polish: Kształtowanie wytłoczek z blach powlekanych). Proceedings of the 14^{th} Scientific and Technological Conference in Metal Forming, Poznań-Czerniejewo, Poland, (2000) 101-107.

[2] W. Gorecki, Engineering of producing and processing of flat metal products (Inżynieria wytwarzania i przetwórstwa płaskich wyrobów metalowych - in Polish). Silesian University of Technology Publishing House, Gliwice –Poland 2006.

[3] E. Dubuisson, P. Lavie, F. Dalard, J.-P. Caire, S. Szunerits, Corrosion of galvanised steel under an electrolytic drop, Corrosion Direct 49 (2007) 910-919.

[4] PN-EN 10147: 2003: Strip and sheet of structural steel hot-dip galvanized in a continuous manner. Technical delivery conditions Taśmy i blachy ze stali konstrukcyjnej ocynkowane ogniowo w sposób ciągły. Warunki techniczne dostawy (in Polish).

[5] PN-EN 10169-1: 1998: Wyroby płaskie stalowe z powłoką organiczną naniesioną w sposób ciągły. Postanowienia ogólne (in Polish).

[6] Y. Hamlaoui, F. Pedraza, L. Tifouti, Corrosion monitoring of galvanised coatings through electrochemical empedance spectroscopy, Corros. Sci. 50 (2008) 1558-1566.

[7] S. Feliu Jr., V. Barranco, XPS stude of the surface chemistry of conventional hot-dip galvanised pure Zn, galvanneal and Zn-Al coatings on steel, Acta Mater. 51 (2003) 5413-5424.

[8] M.A. Arenas, J.J. de Damborenea, A. Medrano, J.-A.Garcia, R Rodriguez, Corrosion behaviour of rare earth ion-implantated hot-dip galvanised steel. Surf. Coat.Tech. 158-159 (2002) 615-619.

[9] A. Amadeh, B. Pahlevani, S. Heshamati-Manesh, Effect of rare earth metal addition on surface morphology and corrosion resistance of hot-dipped zinc coatings. Corr. Sci. 44 (2002) 2321-2331.

[10] M.N.S. Hadi, J. Li, External reinforcement of high strength concrete columns, Composite Structures 65 (2004) 279-287.

[11] Advertising leaflet of the company ArcelorMittal Poland, Department in Świętochłowice (the former „Florian" steel plant).

[12] International Lead and Zinc Study Group (internet: www.ilzg.org).

[13] J. Adamus, Influence of friction on strain nonuniformity during sheet-metal forming (in Polish: Wpływ tarcia na niejednorodność odkształceń przy kształtowaniu blach karoseryjnych), Obróbka Plastyczna, 11/ 1 (2000) 13-19.

[14] W. Gorecki, Z. Sroka, The Influence of Temper Rolling on the Behaviour of the Zinc Coat and Steel Substrate for Hot-dip Galvanized Sheets. Proceedings of the VII Congress on Rolling, Tokio, November 1998.

[15] J. Adamus, The influence of friction and lubrication on the formability of steel sheet and galvanised steel sheet during sheet metal-forming – doctor's dissertation, Technical University of Częstochowa, Poland, (1998) (in Polish).

[16] J. Adamus, M. Gierzyńska-Dolna., Gorecki W., Corrosion Resistance of Galvanised Sheets Used in the Civil Engineering. Proceedings of the 4th International Conference on Contemporary Problems in Architecture and Construction. Sustainable Building Industry of the Future. September 24-27, 2012, Czestochowa, Poland. Edited by J. Rajczyk, A. Pabian, (2012) 599-605.

Advanced Materials Research Vol. 1020 (2014) pp 21-24

doi:10.4028/www.scientific.net/AMR.1020.21

Spectral emissivity of roof membranes and vapor barriers

Miroslav Čekon[1,a], Rastislav Ingeli[2,b]

[1]Institute of Building Structures, Brno University of Technology, Faculty of Civil Engineering, Veveří 331/95, 602 00, Brno, Czech Republic

[2]Department of Building Structures, Slovak University of Technology, Faculty of Civil Engineering, Radlinského 11, 813 68, Bratislava, Slovakia

[a]cekon.m@fce.vutbr.cz, [b]rastislav.ingeli@stuba.sk

Keywords: Spectral emissivity, roof membranes, vapor barriers, infrared spectroscopy

Abstract. Optical parameters become to the features that are currently taken into account more frequently. There are various reasons of dealing with those parameters. Some of them are due to thermal calculation purposes while the other one are trying to consider low-emissivity functions of various innovative building materials. The paper is focused on spectral emissivity analysis of roof membranes and vapor barriers especially that are applied in sloped roofs and walls with air ventilated cavity. The spectral emissivity in the longwave radiation region was assessed by laboratory method of an infrared spectroscopy. The results present courses of spectral nature as well as its transformation into weighted values. As a result the final comparison demonstrates facts of aiming to point out the possibility of receiving any benefit for thermal aspects purpose.

Introduction

Currently, the major emphasis in building energy efficiency is focused on improving the thermal properties of building envelope with various innovative implementations. In research and development of various reflective materials is concentrated on potential for reducing thermal loads in buildings [1] [2]. The radiating heat flow represents in general a negligible proportion of the resulting energy flow within basic requirements to standards for the thermal protection of buildings. Primarily, the main focus is based on typical thermal insulation systems of buildings, but at the same time research trends has led to the progressive development [3] and building envelope innovation. Radiative properties influence of building elements [4] are often neglected in the design of the building envelopes, but these are also significantly involved in the heat transfer and can have an influence for further building physics phenomena, as for instance in their thermal resistance [5].
The basic development requirements for thermal protection of buildings lead to a more stringent standards of improving the thermal performance of the building envelope. Boundary requirements are gradually getting to a level that traditional thermal insulation materials moves to the application of disproportionate thickness or pushes many manufacturers for innovation their proposal elements of the building envelope. It results from the adaptation of these requirements and market needs. The assumptions for the future talk about a significant increase in its thermal characteristics. That is why some innovation tries to employ reflective properties into their nature. Thus currently, the building market and its development are increasingly emerging materials and building elements, which basically seek to involve the mechanisms of thermal radiation. One of the ways in this area is implemented into the reflective application [6] [7] of vapor barriers and roof membrane foils.

Methodical approach and main focus

The main intention of this paper resides in investigating the spectral emissivity properties of roof membranes and vapor barriers that are currently based upon reflective functions, as predominantly compared with its standard version used especially for roof constructions as well as some wall envelopes with air cavity. On the other hand, standard building temperature correlation is evaluated due to its exploratory purpose.

Measurement techniques belonging to emissivity measurements can be divided into calorimetric emission measurements, radiometric emission measurements and reflection measurements [8]. Available principles of determining the spectral emissivity (reflectance) is based on the spectral analysis using infrared spectroscopy in the longwave radiation region. The simplest measurement is based on the integral measurement of the reflected diffusive radiation from the surface implemented by the Fourier transform infrared (FT-IR) spectroscopy also known as Diffuse Reflectance Infrared Fourier Transform (DRIFTS) spectroscopy. Therefore, it is necessary to use an infrared spectrometer in order to experimentally determinate the spectral emissivity ε_λ. There are reflective measurement techniques used [8], which operate on the principle Michaelson wave interferometer and FT-IR. An integrating sphere reflectometer was used for this purpose which was applied into infrared spectrometer Nicolet 380 (Fig. 1a) from the manufacturer Thermo Electron Corporation equipped with an integrating sphere Mid-IR ™ IntegratIR from PIKE Technologies (Fig. 1b) was used. Applied equipment and method predisposes the fact that the results are provided with the best accuracy and spectral sensitivity. This aspect plays an important role for measuring diffuse reflective surfaces. It essentially represents a method by which the detector is able to pick up the whole measurement surface area component of the reflected radiation by gold coated integrating sphere. A diffuse gold reference was used for laboratory testing.

Figure 1. a) FT-IR infrared spectrometer Nicolet 380, b) The integrated sphere Mid-IR ™ IntegratIR cooled with LN2, c) All tested samples

The samples were collected form the most extension building market producer and differentiated into vapor barriers and roof membrane foils (Fig. 1c). The table below (Tab. 1) shows all the tested samples, their description, color and material base. An equivalent diffusion thickness S_d has an important aspect with correlation to the reflective properties in that sense. Both declared values of S_d and emissivity ε are presented in Tab. 1; however the emissivity is given only for reflective ones.

Tab. 1 Table of measured samples

type	description	ε (decl.)	S_d (decl.)	color	sign
vapor barriers	reflective vapor barrier, 170 g/m², matt surface	0.02	300	silver	**S1**
	reflective vapor barrier, 150 g/m², glossy surface	0.43	180	silver	**S2**
	micro perforated foil, 110 g/m²	-	2	translucent	**S3**
	anti-condensation foil, 110 g/m²	-	50	translucent	**S4**
	standard vapor barrier, 110 g/m²	-	40	translucent	**S5**
roof membranes	foil for ventilated wooden casing, 150 g/m²	-	5	black	**S6**
	contact diffuse membrane with insulation function, 200 g/m²	-	0.15	black	**S7**
	contact diffuse membrane with insulation function for ventilated façade layers of opened gaps, 200 g/m²	-	0.20	black	**S8**
	contact diffuse membrane, for ventilated facades, 270 g/m²	-	0.02	black	**S9**
	contact reflective diffuse membrane, 160 g/m²	0.17	0.07	silver	**S10**
	contact diffuse membrane, 160 g/m²	-	0.02	grey	**S11**
	contact diffuse membrane, 210 g/m²	-	0.03	grey	**S12**
	contact diffuse membrane, 150 g/m²	-	0.10	grey	**S13**
	contact diffuse coated membrane, 270 g/m²	-	0.02	grey	**S14**
	contact diffuse membrane, 120 g/m²	-	0.02	grey	**S15**

The results were obtained by the DRIFT method and were authenticated by repetitive measurements of each sample. Spectral curves of the reflectance as a function of the wavelength are presented for spectral range from 2.5 to 20.0 µm. As a result from the law of the conservation of energy and Kirchhoff's laws (1), emissivity can be derived and consequently used for determination of the measurement results in terms of emissivity values.

$$\varepsilon = \alpha = 1 - \rho\,, \qquad \text{or} \qquad \varepsilon_\lambda = \alpha_\lambda = 1 - \rho_\lambda\,, \qquad [-] \tag{1}$$

As a consequence, Plank´s formula (2) of spectral radiance intensity of typical built environment temperatures of 258 K, 273 K, 288 K and 303 K black body $M_{0,\lambda}$ is used as the weighted function for determination of emissivity values for each temperature.

$$M_{0,\lambda}(\boldsymbol{\lambda},T) = C_1 \times \boldsymbol{\lambda}^{5} \times (e^{\frac{C_2}{kT}} - 1)^{1} \qquad [\mathrm{W/(m^2.\mu m)}] \tag{2}$$

As it is well known, the significant region lies somewhere between 8.0 and 15.0 µm in building applications, where all the standard bodies radiate the maximum of its energy. It also represents an area of atmospheric windows where the outdoor conditions are transmissive to thermal radiation.

Results and discussion

The evaluated final results were obtained by DRIFT method. The measured results were authenticated by repeated measurements of each sample. This allowed the precision of various methods and measuring devices to be evaluated. The comparison of multiple measurements of each specimen enabled us to achieve results with negligible deviation and, among others, to simplify the diagrams in showing only one single spectral curve representing one sample. Spectral curves of the reflectance as a function of the wavelength (in spectral range from 2.5 to 20.0 µm) are shown on figures (Fig. 2a and 2b).

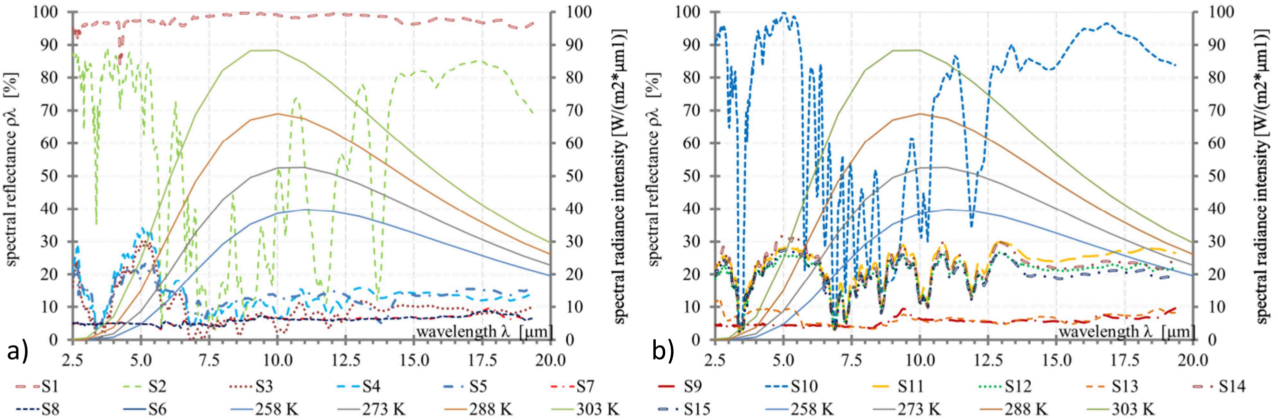

Figure 2. a) Spectral reflectance of the S1 – S8 samples, b) Spectral reflectance of the S9 – S15 samples

The total spectral emissivity values for the whole measured spectrum with respect to spectral irradiance of absolute black body with typical temperature dependence for the practical building application purposes is completely presented in Tab. 2. A percentage expression is presented due to interpret the difference in obtained values; however the range from 0 to 1 is used more frequently.

Table 2 Total spectral emissivity ε_λ as weighted function of temperature in measured infrared spectrum

ε_λ: 2.5 – 18.0 µm	S1 [%]	S2 [%]	S3 [%]	S4 [%]	S5 [%]	S6 [%]	S7 [%]	S8 [%]	S9 [%]	S10 [%]	S11 [%]	S12 [%]	S13 [%]	S14 [%]	S15 [%]
- 15 °C	1.6	57.6	91.6	87.6	87.2	94.9	94.1	94.2	94.6	40.7	77.6	80.2	94.3	78.9	80.7
0 °C	1.7	57.7	91.3	87.2	87.1	95.0	94.2	94.3	94.7	41.1	77.8	80.2	94.3	79.0	80.7
+ 15 °C	1.8	57.6	90.9	86.9	86.9	95.1	94.3	94.4	94.8	41.1	77.9	80.3	94.3	79.0	80.7
+ 30 °C	1.9	57.0	90.5	86.5	86.8	95.2	94.5	94.4	94.8	40.9	78.0	80.3	94.2	78.9	80.6

First and foremost, the results indicate that there are no differences in emissivity values due to temperature impact as a weighted function in final interpretation. The difference occurs only on the third decimal place with consideration of the emissivity range from 0 to 1, what have finally negligible aspect in order to take this impact into account. On the contrary, the differences between the standard foils and those with reflective properties were monitored at certain level. The standard vapor barriers foils (S3, S4, S5) have emissivity values around 0.87, whilst the reflective ones (S1, S2) are with low-emissivity nature (Tab. 2). Reflective foil S1 with relatively matt appearance reaches emissivity around 0.02 and significantly constant progress of spectral curve, which practically corresponds with high equivalent diffusion thickness. It also corresponds with declared value (Tab. 1). On the other hand, reflective foil S2 with glossier surface has emissivity higher than their declared values (0.43) at the level of around 0.57, but significantly filtered in atmospheric window (Fig. 2a). A thin transparent protective layer which reduces the reflective properties of those materials is applied on them. Concerning to the roof membranes foils, the reflective membrane S10 has emissivity around 0.41 whilst its declared value varies around 0.17. Subsequently, samples S6 – S9 and S13 have the same emissivity level at around 0.95, however S11, S12, S14, S15 varies around 0.80.

Conclusion

The paper presents a spectral analysis of the roof membranes and vapor barriers as predominantly an investigation of their emissivity properties due to perform its determination especially for thermal calculation purposes. In addition to that, laboratory methods were used to analyze the spectral emissivity properties of samples in the infrared region, in order to verify their declared values and complete the emissivity parameters absence in non-reflective ones. Finally, a comparison namely of reflective foils with declared values was performed. The results obtained from the infrared spectroscopy, the DRIFT method, demonstrate that there are differences in the spectral emissivity values concerning on their declared values. One of the important connections is strongly specified with air cavity occurrence. Therefore the findings also indicate an appropriate option between non-reflective membranes of receiving some benefit in correlation to thermal aspect of building envelopes; however diffuse parameters seems to be basically more prefered in this area.

This research was supported by the project CZ.1.07/2.3.00/30.0039 of Brno University of Technology and VEGA No. 1/0281/12 research project of Slovak University of Technology.

References

[1] International Energy Agency (IEA), Towards Net Zero Energy Solar Buildings – Fact sheet. SHC Task 40/ECBCS Annex 52 IEA, 2011, pp. 2.

[2] Directive 2010/31/EU of the European Parliament and of the Council of 19 May 2010 on the energy performance of buildings, Official Journal of the European Union, 2010, pp 53.

[3] Labudek J, Oravec P. Energy Solar Wall in Low-Energy Apartment House. Advanced Materials Research. 2013; vol. 649, pp. 155-158. DOI: 10.4028/www.scientific.net/AMR.649.155.

[4] Escudero C, Martin K, Erkoreka A, Flores I, Sala J. M. Experimental thermal characterization of radiant barriers for building insulation. Energy and Buildings, Volume 59, April 2013, Pages 62-72, ISSN 0378-7788

[5] Kalánek J, Šteffek L, Ostrý M. Calculation and Experimental Evaluation of the Thermal Resistance of a Structure with Reflective Insulation. Advanced Materials Research. 2014; vol. 899, pp. 374-380.

[6] Martin J. Tenpierik, Evert Hasselaar, Reflective multi-foil insulations for buildings: A review, Energy and Buildings, Volume 56, January 2013, Pages 233-243, ISSN 0378-7788

[7] Hauser G, Kersken M, Sinnesbichler H., Schade A. Experimental and numerical investigations for comparing the thermal performance of infrared reflecting insulation and of mineral wool, Energy and Buildings, Volume 58, March 2013, Pages 131-140, ISSN 0378-7788,

[8] M.F. Modest, Radiative heat transfer. New York: McGraw-Hill, Inc. 1993, vol. 832, pp.128-145. ISBN 0-07-042675-9.

Advanced Materials Research Vol. 1020 (2014) pp 25-30
© (2014) Trans Tech Publications, Switzerland
doi:10.4028/www.scientific.net/AMR.1020.25

Comparison of experimental and computational characteristics of light perimeter walls of wooden buildings

Marianna Šuštiaková[1, a *], Pavol Ďurica [2,b], Radoslav Ponechal [3,c],
Marek Cangár[4,d]

[1,2,3,4]Faculty of Civil Engineering, University of Žilina, Univerzitna 8215/1, SK-010 26 Zilina, Slovak Republic

[a] marianna.stunova@fstav.uniza.sk, [b] pavol.durica @fstav.uniza.sk,

[c] radoslav.ponechal@fstav.uniza.sk, [d] marek.cangar@fstav.uniza.sk

Keywords: Long time testing measurements, wooden lightweight external walls, temperatures, simulations.

Abstract. The paper evaluated thermo-technical characteristics of the experimental walls, consisting of five different tracks in three different color surfaces at different base material. The hydrothermal behaviour of the structures and layers is monitored year-round. The computational model of the laboratory room and tested samples is compiled and debugged on the basis of experimental measurements. The dynamic simulations of temperature and humidity parameters were realized.

Introduction

Temperatures measurements was made at the lightweight-construction of external wall, which is made in three different material solutions and three different colored exterior side surfaces, is elaborated on the basis temperature measurements made on a sample of the wall built in a climate chamber in the laboratory pavilion type KPSU FCE ŽUŽ (KPSU – Department of Building Constructions and Urban Planning, FCE - Faculty of Civil Engineering, ŽUŽ - University of Žilina). Dimensions of monitored experimental wall are 3670x2670 mm and it comprises five fields. (Table 1). They differ in material composition and colorful surface. First, second, fourth and fifth fields are diffusion sealed construction third field is a diffusion open construction. The composition of wall from the interior to the exterior is as follows: OSB (orientated strand board), PE (poly ethylene) film (except the third field), filling insulation, exterior insulation Hofatex, and thin coating plaster.

The programme ESP-R (an integrated energy modelling tool for the simulation of the thermal, visual and acoustic performance of buildings and the energy use and gaseous emissions associated with associated environmental control systems) was used for thermal simulation. Model in the simulation reproduces reality in a research lab. Its facade is oriented to the south with a rotation of 17 ° to the west. The internal temperature was set according to the values measured temperature of the interior. Was used to simulate the test reference year from IWEC (International Weather for Energy Calculations) database Ostrava and it was selected week that climate data are comparable with recorded climate data.

Course of measured temperatures in construction

Temperatures are recorded at intervals of 30 minutes in a fragment of external wall on the outer surface of the structure, under the plaster under an additional thermal insulation and under the filling thermal insulation. Indoor air temperature was kept 20 ° C and relative humidity was kept at 50% of the chamber, the sample was exposed to actual conditions of external climate from outside. Indoor climate parameters, relative humidity and indoor air temperature was kept by air handling unit. The highest temperatures were measured, as expected, on the surface finish of a grey colour with the lowest reflectance of solar radiation (34%) that absorbs most light radiation, while watching over the temperature on the surface the structure. The third field diffusion open structure has the lowest surface temperature at the time of exposure to the sun from the fields with white finish. The surface temperature of the wall fell below the ambient temperature in all the fields at night during period. Scattering of the measured temperatures during one of the selected day is shown in Fig.1, 6,7

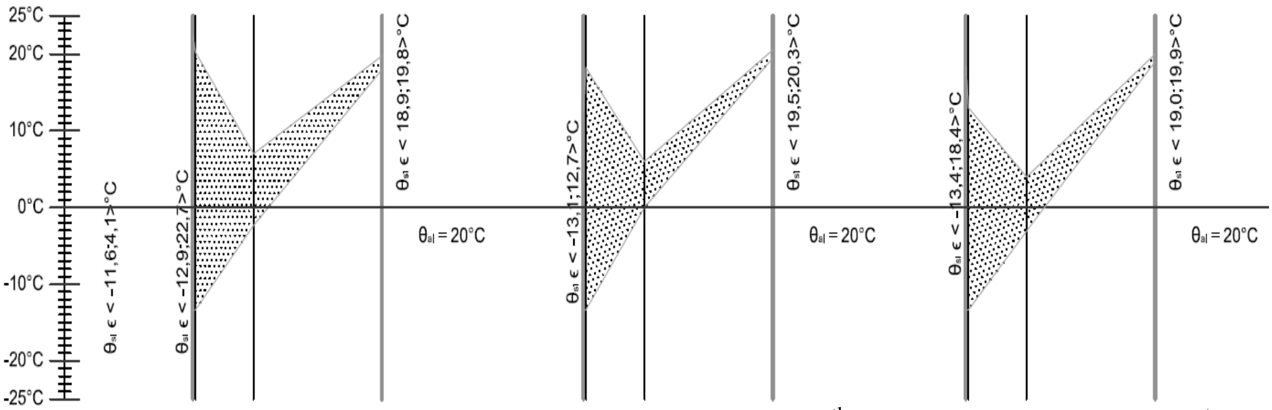

Fig.1 Scattering of the measured temperatures during January 30th 2012, from left to right - 1st field, 3rd field, 4th field.

Thermal simulations

A typical winter day was chosen because of the possibility of comparison measurements of temperatures in the winter with the simulations. Scattering of the measured temperatures in the structure during the day on selected fields 3, 4 and 5 shown in Fig.2 Outdoor conditions during the day were about the same as the date used in the test reference year. The results document the temperature inside each wall structures. On the basis of the results of a simulation of the heat flux, the course of heat transfer coefficients were determined for the different parts of the outer wall (Fig.2, 6, 7). Courses of U-values of the temperature cross-sectional structures (Fig.3) show a significant effect of absorption of solar radiation to heat flow and temperature in the reporting structure.

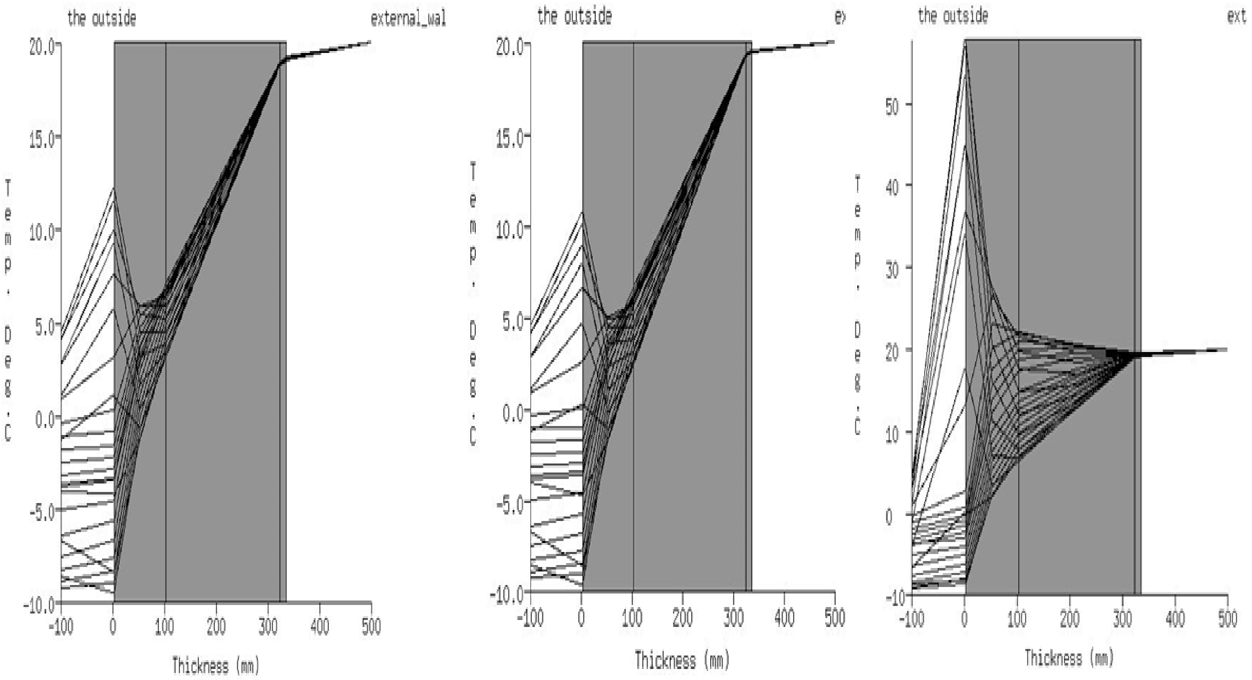

Fig.2 Scattering of the temperatures in construction based on simulation, 3rd field, 4th field and 5th field.

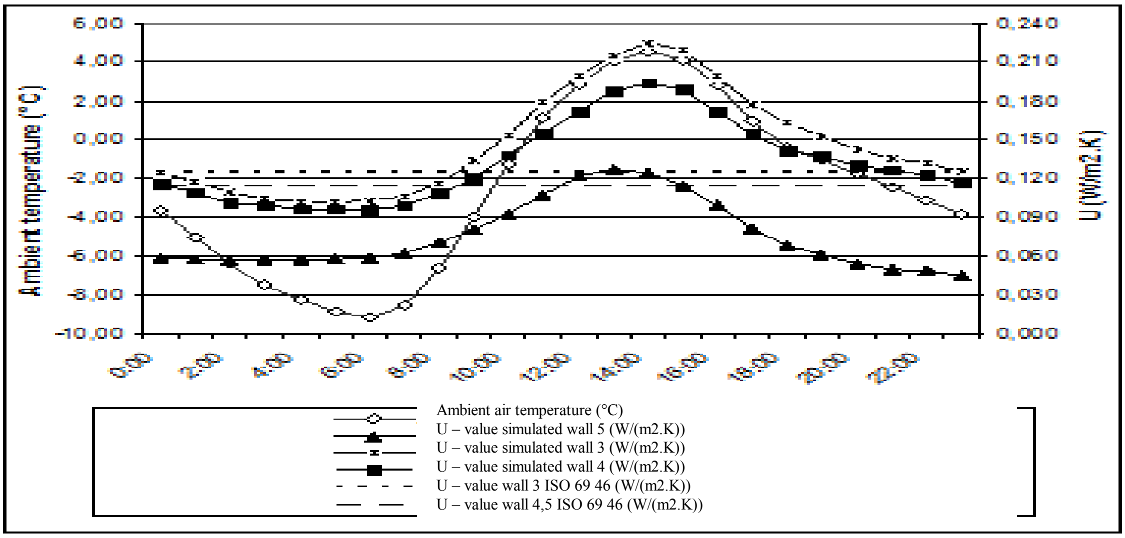

Fig.3 Ambient temperature and U-value courses from simulation.

Thermal balance

The temperature of the outer surface is significantly affected by the incoming solar radiation more than the ambient temperature during the day. Short-wave solar radiation is partly reflected and partly converted into long-wave thermal radiation on impact on non-transparent surface. It is then absorbed by the structure which starts getting heat up. There is a change in the direction of heat flow from the exterior surface towards the interior. As seen in Fig 1, 2, scattering of the temperatures in the construction is also affected by the heat capacity of the materials (Table 1).

Conversely there is a decrease surface temperature below the ambient temperature at night. It is caused by the so-called negative radiation of the night sky. The sky can reach -50 ° C during clear winter nights [5] the emissivity of the night sky is about 74% [6]

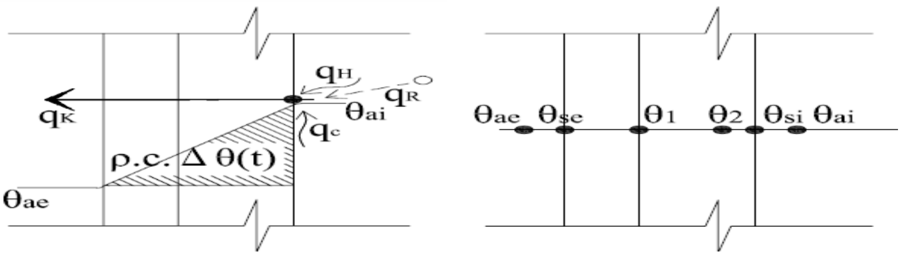

Fig.4 Thermal stability of surface point.

Equations of thermal stability surface point:

$$\rho.c.\Delta\theta_{(t)} = q_{c(t)} + q_{R(t)} + q_{K(t)} + q_{H(t)} \tag{1}$$

Where ρ.c.$\Delta\theta_{(t)}$ - heat accumulated in the construction, $q_{c(t)}$ - convection on the surface (inside / outside), $q_{R(t)}$ - longwave radiation surrounding surfaces, $q_{K(t)}$ - spread one-dimensional heat flow, $q_{H(t)}$ - heat flux from the internal heat source.

Equation of thermal stability of the room during the day:

$$\rho.c.\Delta\theta_{(t)} = q_{sol,t,LW(t)} + q_{R(t)} + q_{K(t)} + q_{H(t)} \tag{2}$$

Equation of thermal stability of the room during the night:

$$\rho.c.\Delta\theta_{(t)} = -q_{r(t)} + q_{R(t)} + q_{K(t)} + q_{H(t)} \tag{3}$$

Table 1 The material characteristic of each field in stationary conditions.

1st. 2nd field

material	description	d	λ	ρ	c	μ	χ	R	$m_x.c_x$
		m	W/(m.K)	kg/m³	J/(kg.K)	-	J/(m².K)	m².K/W	
external plaster	StoSilco	0.004	0.7	1900	720	40	5472	0.01	10725.12
woodfiber board	HofaTex SysTherm	0.1	0.045	210	2100	5	44100	2.22	86436.00
Stone wool insulation	Rockwool MW W	0.22	0.037	40	840	1	7392	5.95	14488.32
vapor layer	Isover Vario KM Duplex	0.00004	1	2000	-	90000		0.00	
								Σ	111649.4
								$\frac{\Delta T}{t}=$	0.005233 K/s
								$\frac{\Delta T}{t}=$	0.00525 K/s

3rd field

material	description	d	λ	ρ	c	μ	χ	R	$m_x.c_x$
		m	W/(m.K)	kg/m³	J/(kg.K)	-	J/(m².K)	m².K/W	
external plaster	StoSilco	0.004	0.7	1900	720	40	5472	0.01	10725.12
woodfiber board	HofaTex SysTherm	0.1	0.045	210	2100	5	44100	2.22	86436.00
Hemp insulation	Cannabest Plus	0,22	0,04	36	1200	1,9	9504	5.50	18627.84
								Σ	115789.0
								$\frac{\Delta T}{t}=$	0.005052 K/s

4th, 5th field

material	description	d	λ	ρ	c	μ	χ	R	$m_x.c_x$
		m	W/(m.K)	kg/m³	J/(kg.K)	-	J/(m².K)	m².K/W	
external plaster	StoSilco	0.004	0.7	1900	720	40	5472	0.01	10725.12
woodfiber board	HofaTex SysTherm	0.1	0.045	210	2100	5	44100	2.22	86436.00
Mineral wool insulatio	Isover ENV	0.22	0.035	24	840	1	4435.2	6.29	8692.99
vapor layer	Isover Vario KM Duplex	0.00004	1	2000	-	90000		0.00	
								Σ	105854.1
								$\frac{\Delta T}{t}=$	0.005513 K/s
								$\frac{\Delta T}{t}=$	0.00555 K/s

The intensity of heat exchange by radiation q_r:

$$q_r = \frac{\sigma\left(T_1^4 - T_2^4\right)}{\frac{1}{\varepsilon_1} + \frac{1}{\varepsilon_2} - 1} = \left[W/m^2\right] \tag{4}$$

Where σ - Stefan-Boltzmann constant, $\sigma = 5{,}67.10^{-8} W/(m^2.K^4)$, T_1, T_2 - surface temperature [K], ε_1, ε_2 - surface emissivity in the range 0-1 (0 ≈ 0%, 1 ≈ 100%). Sunrise was at 7:38 am and the sunset was at 4:41 pm on the selected day [7]. According to Eq. 4 the average intensity of heat exchange by radiation at night was at 1st field 584,26 W/m², 2nd field 586,16 W/m², 3rd field 585,02 W/m², 4th field 583,61 W/m² and 5th field 587,52 W/m². This corresponds to average decrease surface temperature (Table 1, Eq. 5) at 1st field 0,0052°C/s, 2nd field 0,0053°C/s, 3rd field 0,0133°C/s, 4th field 0,0055°C/s and 5th field 0,0056°C/s. Leading to additional heat loss, which are not taken into account in the simulation.

Average decrease surface temperature:

$$\frac{\Delta T}{t} = \frac{q_r}{m.c} = \left[K/s\right] \tag{5}$$

Summary

All fields lightweight perimeter wall are exposed to the same conditions of the interior and the exterior side. Different scattering of the temperatures in the structure is influenced not only by distinct layers of construction, but also natural external influences and different reflectance of solar radiation caused color scheme finishes. The temperature of the outer surface of the structure during the day is particularly influenced by the incoming solar radiation and night is appreciably influenced

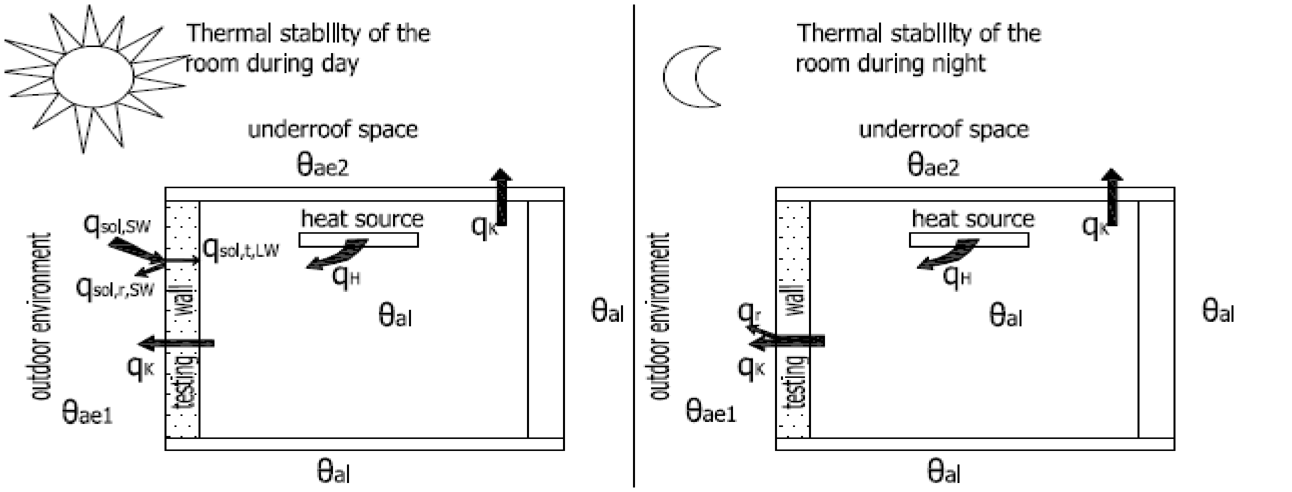

Fig.5 Thermal stability of the room

$q_{r\,(t)}$ - heat transferred from the structure to the environment through the so-called negative radiation, $q_{sol\,(t)}$ - total incident shortwave solar radiation, $q_{sol,r,SW(t)}$ - reflected part of the incident shortwave solar radiation, $q_{sol,t,LW(t)}$ - part of the incident shortwave solar radiation transformed into thermal longwave radiation.

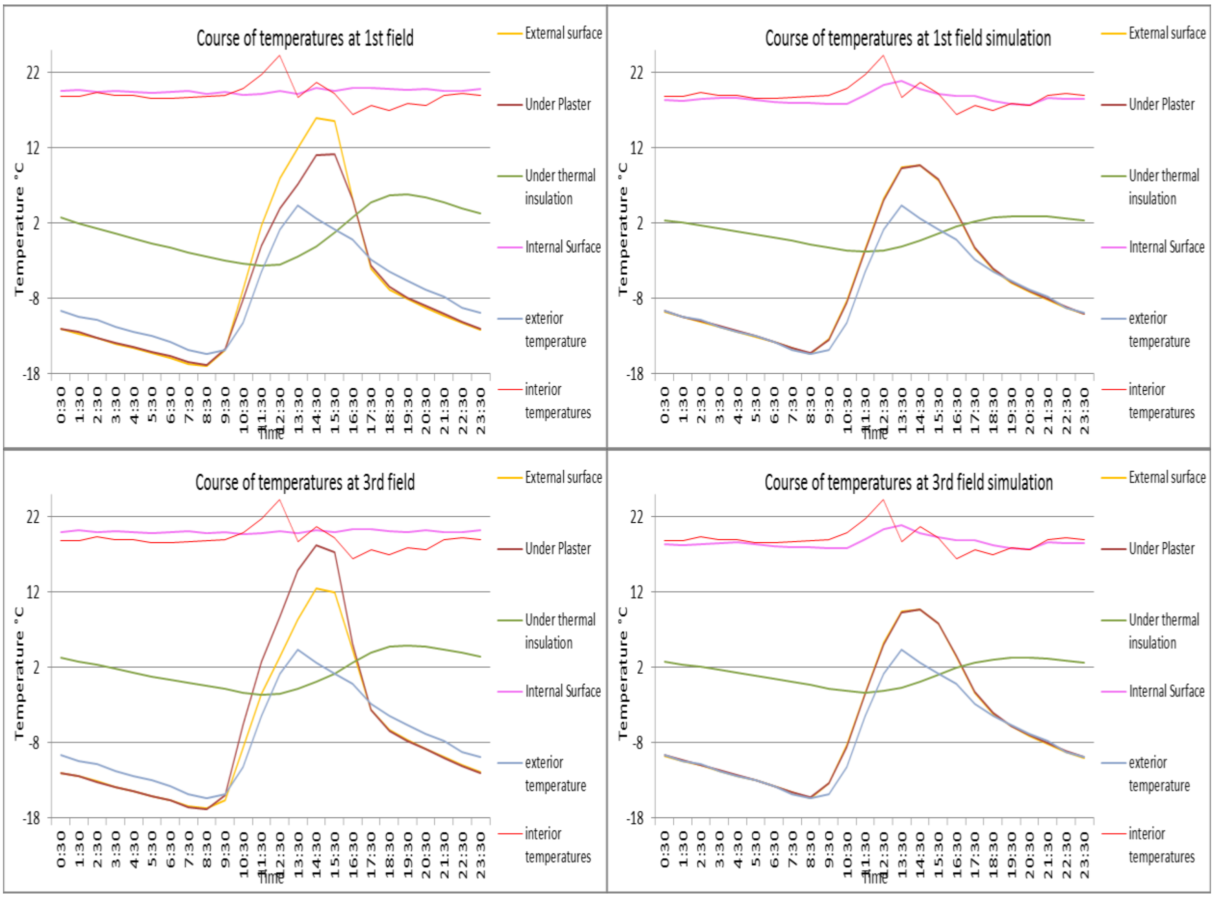

Fig.6 Measured (on the left) and simulated (on the right) temperatures at construction at 30th

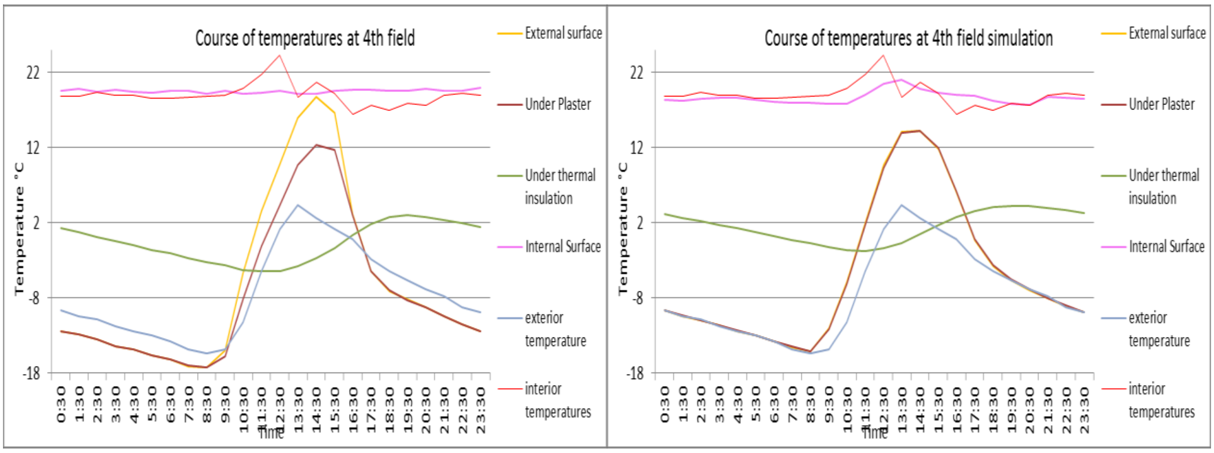

Fig.7 Measured (on the left) and simulated (on the right) temperatures at construction at 30th January 2012.

(on the left) and simulated (on the right) temperatures at construction at 30th January 2012.

by the so called negative radiation of the night sky. In contrast to the effect of solar radiation, effect of negative radiation is not taken into account in the simulation. Negative radiation significantly contributes to total losses at night. Temperature on the inner surface of the structure is more stable, as measured as envisaged simulation. Differences between the temperature at the external surface and temperature under plaster as measured are greater than under simulation (Fig.6, 7). Calculation of heat transfer coefficients showed highly variable non-stationary progressions, significantly different from the fixed standard values. Surprisingly, based on the apparent opposite courses in the midday hours, but the findings in [3], [4].

Acknowledgement

The presented results were obtained with the support of grant projects European Regional Development Fund and Slovak state budget by the projects "Research Centre of the University of Žilina", ITMS 26220220183 and VEGA no. 1/0729/13.

References

[1] I. Chmúrny, Thermal protection of buildings. Bratislava, Jaga Group, 2003, ISBN 8088905273.

[2] M.Štúňová, P. Ďurica, The course of temperatures in construction of lightweight external wall in stationary conditions of the internal environment and the actual conditions of outdoor climate, Konference TRANSCOM Žilina, Slovak Republic, 2013, ISBN 978-80-554-0696-1.

[3] B.R. Anderson, Conventions for U-Value Calculations, IHS - BRE Press. 2006. 2 edition, ISBN 1860819249

[4] B.R. Anderson, The measurement of U-values on site, Information on http://web.ornl.gov/sci/buildings/2012/1985%20B3%20papers/001.pdf

[5] Information on http://plantsinaction.science.uq.edu.au/edition1/?q=content/14-5-2-energy-emission-reradiation

[6] Information on http://www.asterism.org/tutorials/tut37%20Radiative%20Cooling.pdf

[7] data by SHMÚ - Slovak Hydrometeorological Institute

Advanced Materials Research Vol. 1020 (2014) pp 31-36
© (2014) Trans Tech Publications, Switzerland
doi:10.4028/www.scientific.net/AMR.1020.31

Exploration results of applying limestone powder in crushed-stone-sand mixtures for road pavement layers

Hakob Gyulzadyan[1,a], Gevorg Voskanyan[2,b*], Vigen Ter-Simonyan[3,c]
[1]Stepanyan 16/1 apt. 12, Yerevan, RA.
[2]Khanjyan 10, Ararat, RA.
[3]Abovyan 17 apt. 21, Yerevan, RA.
[a]hakob_gyulzadyan@bk.ru, [b]1713gevorg@mail.ru, [c]ardvigen@mail.ru

Keywords: road pavement, crushed stone, sand, limestone, powder, travertine, mixture.

Abstract

This paper presents results of exploration related to C2 and C6 crushed-stone-and-sand ready mixtures strengthened with limestone powder used in road pavement layers.

Limestone powder is an industrial waste, which in Ararat region is in big volumes.

The samples were taken composed of different fractions of crushed-stone and two types of sand produced from crushed basalt and crushed gravel, and were tested. The composition of ready mixtures meets the requirements of corresponding standard on grain size. To these mixtures limestone powder was added of the percentage range 0-30% of the mixture mass.

The main purposes of experimental exploration were to determine the influence of different percentages of limestone powder on compression strength of crushed-stone-and-sand ready mixtures and optimal content of powder. The change of the influence grade was studied by applying different types of sands.

Three cylindrical samples were made for each percentage of limestone powder according to a standard method. Compressive strengths of samples have been determined.

It was concluded, that the applying limestone powder in C2 and C6 ready mixtures contributes to the cohesion of stone grains as well as to obtaining high indicators of compaction in road pavement layers.

The received results allow to arrive to a conclusion that applying limestone powder according to the optimal range distinctly increases the strength characteristics of crushed-stone-sand ready mixtures which in tur contributes the effective implementation of the compacting process. Especially the influence grade is considerable in C6 ready mixtures containing a large amount of crushed stone, as well as in mixtures using sands with smaller fineness modulus.

1. Introduction

Nowedays in road construction technology stone materials are widely used for road pavement layers as far as a good experience for applying such materials has been lately accumulated. The crushed stone-sand-gravel mixtures (hereinafter called ready mixtures) have been developed and defined, which are widely used in RA recent years. It is possible to reach to higher compacting indices in layers from this mixtures. Specifications of ready mixtures are defined by standard GOST 25607-2009 [1]. They are classified to C1-C11 types. The regularities of processing ready mixtures with inorganic binders are defined by standard GOST 23558-94 [2]. There are known technologies of applying different types of materials from industrial wastes and slag in road pavement layers [3,4,5].